UNIVERSITY OF CALIFORNIA
RIVERSIDE

New Interactions in Effective Theory

A Dissertation submitted in partial satisfaction
of the requirements for the degree of

Doctor of Philosophy

in

Physics

by

Kyungwook Kim

March 2011

Dissertation Committee:

Dr. Jose Wudka, Chairperson
Dr. Ernest Ma
Dr. John Ellison

The Dissertation of Kyungwook Kim is approved:

Committee Chairperson

University of California, Riverside

Acknowledgments

I am very happy to have the opportunity to thank those who made this work possible. First of all, I would like to express my sincere appreciation to my advisor Prof. Jose Wudka for all his help in my research and in writing this dissertation. Without his help, I would not have finished this thesis successfully. He reviewed my dissertation extensively, and gave me useful and important advice.

I am very grateful to my dissertation committee members Prof. Ernest Ma and Prof. John Ellison for not only serving in my committee, but for their helpful comments in the final exam. I also would like to thank my collaborators in my first paper, as well as Professor Clare and Professor Hanson in our department for helpful discussions about high energy experiments. My thanks go out also to Will, Herb, and Jack for their help when I was a TA. I would like to thank Lucy in the payroll office for her kind help in many occasions.

My colleagues in the department of physics and astronomy, in particular my office mates at UCR were extremely helpful in assisting me with my research. I will always remember the time with my friends who are very special to me. My dear friend Henry and his wife Ling helped me whenever the need was there. Hsiang-Ku and Peng, and Mayra helped me in any possible way and any occasion. Especially, Mayra helped me with English so many times and Hsiang-Ku tried to help me so much that I felt them as my real sisters. I miss our dear big sister Hulya whose help I can still count on without any hesitation. I thank my academic brother Ricardo for many valuable discussions on physics. Joyful and helpful discussions with Vincent, Dundar and Nick made me happy and wise.

I always remember what I learned from my first academic advisor Prof. Young-

Jae Lee. He encouraged me to continue in physics and taught me how to study, how to teach, and the importance of research. I miss my academic brothers and sisters who were students of Professor Lee.

To my wife, Yongju, I send my deepest appreciation and love. She sacrificed herself for me and has been raising our most precious daughter and son with love. I also would like to express my boundless love and gratitude to my daughter, Alison, and my son, Andrew who made me always happy.

I also would like to send my sincere respect and appreciation to my parents in law for their support and love to my family. I also thank my sister and brother in law who treated me as their real elder brother and helped my family when we stayed in Korea.

I would like to express my unlimited gratitude and love to my parents who gave birth to, raised and supported me with endless love. I am also grateful to my only brother and my best friend Kyunghwan. I am very much indebted to Youngmin who brought health to my mother. I would like to send my love and thanks to my maternal grandparents of Nah-ah-ree who loved me more than anyone. I also would like to send my sincere love to my aunts and uncles, and all my cousins who have loved me always.

Lastly, I dedicate my dissertation to my grandparents of Mah-cha-ree, who gave me endless love and taught me the most important thing in my life, love.

To my grandfather of Mah-cha-ree

ABSTRACT OF THE DISSERTATION

New Interactions in Effective Theory

by

Kyungwook Kim

Doctor of Philosophy, Graduate Program in Physics
University of California, Riverside, March 2011
Dr. Jose Wudka, Chairperson

I studied the physics beyond the Standard Model by using effective field theory. I built models of new heavy physics and obtained their low energy effective Lagrangians; I studied new effects on physical observables in collider experiments and nuclear, astrophysical and cosmological processes. In Part 1, I will discuss the phenomenology of the most general effective Lagrangian including up to dimension five operators built with standard model fields and right-handed neutrinos. In particular, the new interactions by a dimension five electro-weak moment operator of right-handed neutrinos will be shown mainly. In Part 2, new interactions for neutrinoless double beta ($0\nu\beta\beta$) decay will be discussed. The observation of the $0\nu\beta\beta$ decay will (i) tell us the type of neutrinos (Majorana or Dirac); (ii) open up the possibility of new physics; (iii) provide the constraints on the energy scales of the new heavy physics. I will list the effective operators and possible new physics models contributing to the $0\nu\beta\beta$ decay. Then I will present the condition for the dominant contribution of each effective operator over other operators, the lower limits on the energy scales of the new physics models, and the types of heavy particles that can contribute to the $0\nu\beta\beta$ decay and may also be produced at the LHC.

Contents

List of Figures

List of Tables

Part I

Right-handed neutrino magnetic moments

Chapter 1

Introduction

In Part 1, I will discuss the phenomenology of the dimension five effective operators including right-handed neutrinos. This work was published on Physical Review D in 2009 [1] by Alberto Aparici, Kyungwook Kim, Arcadi Santamaria, and Jose Wudka. In the following section an introduction to the effective field theory will be given, which is one of the most efficient tools to describe the physics beyond the Standard Model.

1.1 Effective field theory

Effective field theory is a tool to describe the physics of elementary particles with an energy scale above the Standard Model and below the mass scale of the heavy particles in new heavy physics which we do not know the details. The effective theory is described by effective Lagrangian that provides a parameterization of virtual heavy physics effects. In this section, I will follow the ref. [2], in which an introduction to effective theory is given.

1.1.1 Effective Lagrangian

To construct a model for a certain set of phenomena, first we need to determine the corresponding fields for the light particles. Second, we need to specify low-energy symmetries of the model based on the experimental evidence. Finally, we can construct the most general Lagrangian with the fields satisfying the symmetries.

Since we need an effective theory describing the physics at energy scale below a certain level Λ (the energy scale of new physics) the effective action S_{eff}^{Λ} for the theory will be obtained by integrating the action of the corresponding full theory over all Fourier components of energy $\geq \Lambda$ and all fields of masses above Λ. Then the effective Lagrangian, $\mathcal{L}_{\text{eff}}$ can be defined in the effective action as follows

$$S_{\text{eff}}^{\Lambda} = \int d^4x \mathcal{L}_{\text{eff}} = \int d^4x \sum_i \alpha_i(\Lambda)\mathcal{O}_i, \tag{1.1}$$

where $\mathcal{O}_i$ are effective operators consist of only low energy fields and α_i are Λ-dependent coefficients. The effective Lagrangian describes all the virtual effects of heavy physics. The form of the effective Lagrangian is independent of the model of new physics and provides consistent, complete and unitary description of heavy physics effects at scales below Λ. In this thesis, we will assume that in all the theories we consider, the heavy physics is weakly-coupled and decoupling. This means that, if we define $\mathcal{L}^{(4)}$ as part of $\mathcal{L}_{\text{eff}}$ containing operators of dimension less than four, $\mathcal{L}^{(4)}$ is renormalizable. Then all new-physics effects disappear in the limit $\Lambda \to \infty$, so the coefficients α_i can be expanded in powers of $1/\Lambda$.

1.1.2 Symmetries of effective theory

Since the energy level of heavy physics Λ is greater than the energy level of electroweak symmetry breaking, we impose the same gauge invariance on the effective

theory as the Standard Model has. However, we do not need to impose global symmetries such as lepton or baryon number conservations because they are accidental symmetries of the Standard Model.

1.1.3 Redundancy of effective operators

Effective operators can be removed from the effective Lagrangian if the S matrix does not change by replacing the effective operators by others or linear sum of other operators. This is the case when operators are related by the equations of motion [3].

1.1.4 Estimations of the effective operator coefficients

We can estimate the coefficient of an effective operator from the new physics generating the effective operator. The estimation depends on whether the corresponding new physics is weakly or strongly coupled theory. If an effective operator is generated from a weakly coupled new physics at tree level the coefficient estimate is,

$$\alpha_i \sim \frac{1}{M_{\rm NP}^{d-4}} \tag{1.2}$$

where $M_{\rm NP}$ is the energy scale of the new physics and d is the energy-dimension of the effective operator. If an effective operator can only be generated at one-loop level then the coefficient estimate will be further suppressed by a factor of $1/16\pi^2$.

If an effective operator is generated by a strongly coupled theory, the coefficient is estimated as follows [2, 4]

$$\alpha_i \sim \frac{\Lambda^{4-A-3B/2-C-D}}{(4\pi)^{2-A-B}}, \tag{1.3}$$

where A, B, C, and D are the number of scalar fields, the number of fermion fields, the number of derivatives, and the number of gauge fields in the effective operator respectively.

1.2 Neutrino physics

In this section, I will give a brief introduction to neutrinos and their non-zero masses following [5, 6] and the references therein.

1.2.1 Discovery of neutrinos

The discovery of neutrinos was from the observation of the decay processes of nuclei

$$N(A, Z) \to N'(A, Z \pm 1) + e^{\mp}, \tag{1.4}$$

where N and N' are the initial and final nuclei. In the above processes the total energy E_e of the emitting electron is approximately the difference between the initial and the final masses of the nuclei

$$E_e \sim M_N - M_{N'} \equiv Q. \tag{1.5}$$

However, the experimental result for E_e was different from the expectation. The electron's total energy varied continuously between electron's rest mass and Q. Pauli suggested that a neutral fermion with spin 1/2 should be emitted together with an electron to explain the observation. This idea was developed by Fermi, and he invented the effective theory of weak interaction. Fermi's theory predicted the decay rates of neutron and muon, and also predicted the smallness of the neutrino's cross-section. By year 2000, the existence of all three neutrinos have been experimentally proved.

1.2.2 Evidence for non-zero neutrino mass

Whether or not neutrinos are massive the created neutrino through a weak interaction

$$-\mathcal{L} = \frac{g}{\sqrt{2}} \bar{\nu}_L \gamma^\mu e_L W_\mu^+ + \text{H.c.} \tag{1.6}$$

is a flavor eigenstate, where the constant g is a gauge coupling constant, ν_L and e_L are flavor eigenfields of left-handed neutrino and left-handed electron, and $W_\mu^\pm$ are the charged weak bosons. If neutrinos are massive, then the flavor eigenstate created through the above interaction will, in general, be a linear combination of mass eigenstates

$$|\nu_\alpha\rangle = \sum_{i=1}^{n} U_{\alpha i}^* |\nu_i\rangle, \tag{1.7}$$

where n is the number of the generations of neutrinos and U is the mixing matrix between charged left-handed leptons and left-handed neutrinos in flavor space. If $n = 3$ then U can be parameterized as

$$U = \begin{pmatrix} 1 & 0 & 0 \\ 0 & c_{23} & s_{23} \\ 0 & -s_{23} & c_{23} \end{pmatrix} \begin{pmatrix} c_{13} & 0 & s_{13}e^{-i\delta} \\ 0 & 1 & 0 \\ -s_{13}e^{i\delta} & 0 & c_{13} \end{pmatrix} \begin{pmatrix} c_{21} & s_{12} & 0 \\ -s_{12} & c_{12} & 0 \\ 0 & 0 & 1 \end{pmatrix} \begin{pmatrix} e^{i\eta_1} & 0 & \\ 0 & e^{i\eta_2} & 0 \\ 0 & 0 & 1 \end{pmatrix}, \tag{1.8}$$

where $s_{ij} \equiv \sin\theta_{ij}, c_{ij} \equiv \cos\theta_{ij}$ and δ, η_i are phases. η's appear only for Majorana neutrinos and cannot be measured in neutrino oscillation experiments. The Majorana phases can be measured in experiments for neutrinoless double beta decay which will be treated in Part 2 of this thesis.

1.2.2.1 Neutrino oscillations in vacuum

As a flavor eigenstate of neutrino travels the space, each mass eigenstate will evolve differently depending on its energy. For simplicity, let us consider the case that $n = 2$ and use the standard approximation that the mass eigenstates are momentum eigenstates. Then the flavor eigenstates at time t and at the distance l from where the neutrino was created will be as follows,

$$\begin{pmatrix} |\nu_\alpha, t, l\rangle \\ |\nu_\beta, t, l\rangle \end{pmatrix} = \begin{pmatrix} \cos\theta & \sin\theta \\ -\sin\theta & \cos\theta \end{pmatrix} \begin{pmatrix} e^{-i(E_1 t - p_1 l)}|\nu_1\rangle \\ e^{-i(E_2 t - p_2 l)}|\nu_2\rangle \end{pmatrix} \tag{1.9}$$

where ν_1 and ν_2 are mass eigenstates with $m_1 \leq m_2$. Without loss of generality the mixing angle θ can be taken as $0 \leq \theta \leq \pi/2$, and it can be assumed that the neutrino propagates in vacuum or not very dense matter. If neutrinos are light enough to be relativistic, and have the same momentum p then

$$E_i \sim p + \frac{m_i^2}{2E},\ l \sim t, \tag{1.10}$$

and, omitting an overall phase, (1.9) will be approximately

$$\begin{pmatrix} |\nu_\alpha, l\rangle \\ \\ |\nu_\beta, l\rangle \end{pmatrix} = \begin{pmatrix} \cos\theta & \sin\theta \\ \\ -\sin\theta & \cos\theta \end{pmatrix} \begin{pmatrix} e^{-im_1^2 l/2E}|\nu_1\rangle \\ \\ e^{-im_2^2 l/2E}|\nu_2\rangle \end{pmatrix}. \tag{1.11}$$

As a result neutrinos oscillate between their flavor states as they travel, and from the above equation, the probability that α-flavor eigenstate becomes β-flavor eigenstate is

$$P_{\alpha\beta} = \langle \nu_\alpha | \nu_\beta, l\rangle = \sin^2 2\theta \sin^2 \phi_{21}, \tag{1.12}$$

where

$$\phi_{ji} \equiv \frac{\Delta m_{ji}^2 l}{4E},\ \Delta m_{ji}^2 \equiv m_j^2 - m_i^2, \tag{1.13}$$

in natural units, in which $c = \hbar = 1$ and in more practical units for experimental observations,

$$\phi_{ji} = 1.3 \Delta m_{ji}^2 \frac{l}{E} \frac{\text{MeV}}{\text{eV}^2 \cdot \text{m}}, \tag{1.14}$$

where Δm^2 is in eV^2, l is in meters, and E is in MeV. The survival probability can be easily obtained as

$$P_{\alpha\alpha} = 1 - P_{\alpha\beta}. \tag{1.15}$$

From (1.14), if the neutrino oscillation is observed we can conclude that at least one flavor of neutrinos has non-zero mass.

Since neutrinos have small masses, Δm^2 is also small. Therefore, to have non trivial value for the oscillation probability, l/E in (1.12) has to be large enough such

that

$$\phi_{21} \gtrsim \frac{\pi}{2}. \tag{1.16}$$

When l is very large we can take the average value of $\sin^2\phi_{21}$ as 1/2. We are going to use this throughout the chapter. l/E is different in various experiments. For solar neutrino experiments, the distance l from the sun to the detector on the earth is about 10^{11} m and $E \sim$ MeV so the experiments can probe Δm^2 down to 10^{-11} eV^2. Long baseline reactor experiments have $l \sim 10^5$ m and $E \sim$ MeV so Δm^2 can be probed down to 10^{-5} eV. For atmospheric experiments $l \sim 10^4$ km and $E \sim$ GeV so Δm^2 can be probed down to 10^{-4} eV. A long baseline accelerator experiment has $l \sim 10^3$ km and $E \sim$ GeV so Δm^2 can be probed down to 10^{-3} eV.

1.2.2.2 Atmospheric neutrino oscillation

In the earth's atmosphere, π and K mesons are created in the collisions of high energy cosmic rays with nuclei. The produced mesons decay dominantly into $\mu^+(\mu^-) + \nu_\mu(\bar{\nu}_\mu)$ through the Standard Model weak coupling because, in the rest frame of the π or K meson, decaying into relativistic $e^+(e^-) + \nu_e(\bar{\nu}_e)$ is not allowed by angular momentum conservation. Super-Kamiokande (SK) experiment [7] detected clearly fewer number of ν_μ compared to the expected number from the known cosmic ray fluxes without neutrino oscillations. This ν_μ-deficit indicates $\nu_\mu - \nu_\tau$ oscillation. The data from the SK showed that the survival probability

$$P_{\mu\mu} = 1 - \sin^2 2\theta_{\rm atm} \sin^2 \phi_{\rm atm}, \tag{1.17}$$

where

$$\phi_{\rm atm} \equiv 1.3 \Delta m^2_{\rm atm} \frac{l}{E} \frac{\rm MeV}{\rm eV^2 \cdot m}, \tag{1.18}$$

$$\Delta m^2_{\rm atm} \equiv (\text{heavier mass eigenvalue})^2 - (\text{lighter mass eigenvalue})^2, \tag{1.19}$$

was minimum when $l/E \sim$ 500km/GeV. This means

$$1.3\Delta m^2_{\rm atm} 500 \frac{\rm km}{\rm GeV} \frac{\rm MeV}{\rm eV^2 \cdot m} = \frac{\pi}{2}. \tag{1.20}$$

From this we can obtain

$$\Delta m^2_{\rm atm} = 2.4 \times 10^{-3}\ {\rm eV}^2. \tag{1.21}$$

Also, from the observation of large oscillation

$$\sin^2 2\theta_{\rm atm} \sim 1, \tag{1.22}$$

which means

$$\theta_{\rm atm} \sim \frac{\pi}{4}. \tag{1.23}$$

The above two results agreed with two long-baseline accelerator experiments K2K [8] and MINOS [9]. The lepton mixing angle is very large when it is compared to the mixing angle in quark sector, and therefore it is not as obvious how to assign each neutrino mass eigenvalue to each flavor eigenstate as in the quark sector.

1.2.2.3 Neutrino oscillations in matter

When neutrinos are in a dense matter the Hamiltonian will include potential energy terms in addition to the kinetic energy terms. The potential is generated by the charged weak interaction of neutrinos with the matter. This will affect the neutrino oscillation significantly if the neutrino interaction in matter is coherent and forward scattering, which means that the neutrinos have the same momentum and spin before and after the interaction. The effect of the effective potential on the neutrino oscillation is known as MSW effect [10,11]. Let us consider the case that ν_e is traveling in a medium with electrons, protons and neutrons. Then from the wave equation, the neutrino mixing in the matter can be calculated, and the flavor eigenstates created at x can be expressed

as [6]

$$\begin{pmatrix} \nu_\alpha \\ \nu_\beta \end{pmatrix} = \begin{pmatrix} \cos\theta_m & \sin\theta_m \\ -\sin\theta_m & \cos\theta_m \end{pmatrix} \begin{pmatrix} \nu_{m_1} \\ \nu_{m_2} \end{pmatrix}, \tag{1.24}$$

$$\tan 2\theta_m \equiv \frac{\Delta m^2 \sin 2\theta}{\Delta m^2 \cos 2\theta - A}, \tag{1.25}$$

$$A \equiv 2\sqrt{2} G_F E[n_\alpha(x) - n_\beta(x)], \tag{1.26}$$

where $\nu_{m_{1,2}}$ are mass eigenstates in matter, and $n_{\alpha(\beta)}(x)$ is the density of neutrino $\alpha(\beta)$ at x. When $A = 0$ then $\theta_m = \theta$. For $A > A_R \equiv \Delta m^2 \cos 2\theta$, if $\theta < \pi/4$, the mass eigenstate in the matter will have inverted flavor components compared to the mass eigenstates in vacuum. Therefore, when a neutrino mass eigenstate in matter is passing across the region where $A = A_R$, flavor components will be switched. This is called level crossing.

The mass eigenstates of neutrinos in matter are not energy eigenstates. However, if the matter potential is a slowly varying function of position then the mass eigenstates in matter are approximately mass eigenstates, which is the adiabatic transition approximation. In this case, the oscillation probability can be expressed as [6]

$$P_{\alpha\beta} = \left| \sum_{i=1}^{2} \tilde{U}_{\alpha i} U_{\beta i} \exp\left\{ -\frac{i}{2E} \int_0^l m_i^2(x) dx \right\} \right|^2, \tag{1.27}$$

where

$$\tilde{U} \equiv \begin{pmatrix} \cos\theta_m & \sin\theta_m \\ -\sin\theta_m & \cos\theta_m \end{pmatrix}, \; U = \begin{pmatrix} \cos\theta & \sin\theta \\ -\sin\theta & \cos\theta \end{pmatrix}, \tag{1.28}$$

m_i are the masses of the eigenstates in matter and the integration is performed along the path of the neutrinos.

1.2.2.4 Solar neutrino oscillation

The electron density in the sun decreases monotonically and slowly from its center to surface. Therefore (1.27) can be used to analyze the neutrino oscillation in the

sun, and the survival probability at detectors on the earth can be rewritten as

$$P_{ee} = \cos^2\theta_m \cos^2\theta_{\rm sol} + \sin^2\theta_m \sin^2\theta_{\rm sol} + \frac{1}{2}\sin^2 2\theta_m \sin^2 2\theta_{\rm sol} \cos\left[\frac{1}{2E}\int_0^l dx\{m_2^2(x) - m_1^2(x)\}\right], \tag{1.29}$$

where $\theta_{\rm sol}$ is a mixing angle of U in (1.28), and we choose to use the convention of positive Δm^2 and $0 \leq \theta_{\rm sol} \leq \frac{\pi}{4}$. Then the last term is averaged to zero for the sun giving

$$P_{ee} = \frac{1}{2}(1 + \cos 2\theta_m \cos 2\theta_{\rm sol}). \tag{1.30}$$

In the above equation $\cos 2\theta$ is always positive, and therefore whether P_{ee} is greater than $1/2$ depends on the sign of $\cos 2\theta_m$, which depends on the sign of the denominator of (1.25), $A_R - A$.

If $A \ll A_R$ then $\theta_m \sim \theta_{\rm sol}$ and the survival probability on the earth will be the same as in vacuum (1.12) with $\sin^2\phi$=1/2 because of the long l.

If $A \lesssim A_R$

$$P_{ee} > \frac{1}{2}. \tag{1.31}$$

Since P_{ee} implies no flavor change, the above equation means that most neutrinos will be electron-like when they get to the Earth.

If $A > A_R$ then

$$\cos 2\theta_m \cos 2\theta_{\rm sol} < 0 \rightarrow P_{ee} < \frac{1}{2}. \tag{1.32}$$

For example, if $A \gg A_R$ then

$$\theta_m = \frac{\pi}{2} \rightarrow P_{ee} = \sin^2\theta_{\rm sol}, \tag{1.33}$$

which resolves the solar neutrino problem that we observe less ν_e than we expected without taking account of MSW effect.

The electron density and adiabatic condition in the sun leave four independent solutions for $\Delta m_{\rm sol}$ and $\sin^2 2\theta_{\rm sol}$. They are SMA (Small Mixing Angle), LMA (Large Mixing Angle), LOW (Low Mass), and VAC(Vacuum Oscillation). By comparing the experimental results from SK, SNO [12, 13], KamLAND [14–16] and the predicted survival probabilities [8] for the four different solutions, all other solutions have been ruled out but the LMS solution. The best fit value for the solar neutrino oscillations were

$$\Delta m^2_{\rm sol} = 7.7 \times 10^{-5} eV^2, \ \sin^2\theta_{\rm sol} = 0.33. \tag{1.34}$$

1.2.3 Neutrino mass hierarchy and the lepton mixing matrix

From the various neutrino oscillation experiments, $\Delta m^2_{\rm atm}$ and $\Delta m^2_{\rm sol}$ were found, and also it is found that $\Delta m^2_{\rm atm} > \Delta m^2_{\rm sol}$ between neutrino mass eigenvalues. Assuming there are only three mass eigenvalues, we still do not know if $\Delta m^2_{\rm sol}$ is the gap between the lightest two mass eigenvalues or the heaviest two. If we define Δm_{ij} and θ_{ij} as the mass-squared difference and the mixing angle between two mass eigenstates ν_i and ν_j, and $\Delta m^2_{\rm sol} = \Delta m^2_{21}$ then from the reactor experiment CHOOZ [17], it was found that

$$\sin^2\theta_{13} \leq 0.07. \tag{1.35}$$

This means that ν_e component of ν_3 is very small and therefore we can conclude that $\theta_{\rm sol} \cong \theta_{12}$, $\theta_{\rm atm} \cong \theta_{23}$, $\Delta m^2_{\rm sol} = \Delta m^2_{21}$, and $\Delta m^2_{\rm atm} = \Delta m^2_{32}$.

For the case there are only three neutrino mass eigenvalues, from the known mixing angles and the unitarity of the lepton mixing matrix, the ranges of the elements

of the absolute value of U in (1.8) have been obtained in [6, 18] at 90% CL

$$|U| = \begin{pmatrix} .80 \sim .84 & .53 \sim .60 & .00 \sim .17 \\ .29 \sim .52 & .51 \sim .69 & .61 \sim .76 \\ .26 \sim .50 & .46 \sim .66 & .64 \sim .79 \end{pmatrix}. \tag{1.36}$$

1.2.4 Physics models for massive neutrinos and the see-saw mechanism

In the Standard Model, after the spontaneous breaking of $SU(2)$ symmetry, fermions acquire masses through the Yukawa interaction terms. Each fermion mass is Yukawa coupling constant times the vacuum expectation value of the scalar fields $v/\sqrt{2} = 174$ GeV. A Yukawa term consists of a pair of $SU(2)$ doublets of a scalar and a left-handed fermion, and a right-handed fermion singlet. The matter content of the Standard Model does not include right-handed neutrinos, which does not allow neutrinos to have masses.

Since we have been obtaining the information that neutrinos are massive and also their masses are very small compared to the charged fermions, we need new physics allowing neutrinos to have masses much smaller than the vacuum expectation value. In effective field theory, if we include the matter content with n additional right-handed neutrinos and the local symmetries of the Standard Model, we can have the following mass terms after the spontaneous symmetry breaking

$$\mathcal{L}_{m_\nu} = -\bar{\nu}_L M_D \nu_R - \frac{1}{2}\overline{\nu_R^c} M_R \nu_R - \frac{1}{2}\overline{\nu_L^c} M_L \nu_L + \text{H.c.}, \tag{1.37}$$

where M_D, M_R, and M_L are mass matrices in the flavor space and are called Dirac, Right-handed Majorana, and left-handed Majoran mass term respectively. M_D is a completely general $3 \times n$ matrix, M_R is a complex symmetric $n \times n$ matrix, and M_L is a complex symmetric 3×3 matrix. The Dirac mass term is from a Yukawa interaction, the right-handed neutrino mass term can be put either by hand or through effective

operators, and the left-handed neutrino mass term can be generated only by effective operators, the lowest dimension one is unique:

$$\mathcal{L}_{\text{eff}} = \bar{\bar{\ell}}\phi\chi\tilde{\phi}^{\dagger}\ell + \text{H.c.}, \tag{1.38}$$

where χ is a complex symmetric 3×3 flavor matrix and have energy dimension, -1. This dimension five operator was first introduced by Weinberg [19]. The neutrino mass terms in (1.37) can be rewritten in a convenient form as

$$\mathcal{L}_{m_\nu} = -\frac{1}{2}\left(\bar{\nu}_L \;\; \overline{\nu_R^c}\right)\begin{pmatrix} M_L^{\dagger} & M_D \\ M_D^T & M_R \end{pmatrix}\begin{pmatrix} \nu_L^c \\ \nu_R \end{pmatrix} + \text{H.c.} \tag{1.39}$$

If $M_R = M_L = 0$, then neutrinos will have usual Dirac masses as charged fermions. However, the Dirac mass, which is proportional to the coefficient of the Yukawa coupling of the neutrinos times $v/\sqrt{2}$, can be made small only if the Yukawa coupling is extremely small.

If the scales of the eigenvalues of the mass matrices are

$$M_R \gg M_D \gg M_L, \tag{1.40}$$

then the symmetric neutrino mass matrix can be approximately diagonalized by a unitary matrix as follows

$$\begin{aligned}\mathcal{L}_{m_\nu} &= -\frac{1}{2}\left(\bar{\nu}_L \;\; \overline{\nu_R^c}\right) V^* V^T \begin{pmatrix} M_L^{\dagger} & M_D \\ M_D^T & M_R \end{pmatrix} V V^{\dagger} \begin{pmatrix} \nu_L^c \\ \nu_R \end{pmatrix} + \text{H.c.} \\ &\simeq -\frac{1}{2}\left[(\bar{\nu}_L - \overline{\nu_R^c}\varepsilon^{\dagger})U_\nu \;\; (\bar{\nu}_L\varepsilon + \overline{\nu_R^c})V_N^*\right] D_\nu \begin{bmatrix} V_\nu^T(\nu_L^c - \varepsilon^*\nu_R) \\ V_N^{\dagger}(\varepsilon^T\nu_L^c + \nu_R) \end{bmatrix} + \text{H.c.},\end{aligned} \tag{1.41}$$

where

$$V \simeq \begin{pmatrix} U_\nu^* & M_D^* M_R^{-1} U_N^* \\ -M_R^{-1} M_D^T U_\nu^* & U_N \end{pmatrix} \tag{1.42}$$

is the $(3+n)\times(3+n)$ unitary matrix in flavor space diagonalizing the mass matrix,

$$\varepsilon \equiv M_D M_R^{-1}, \tag{1.43}$$

and

$$D_\nu \simeq \begin{bmatrix} U_\nu^\dagger (M_L^\dagger - M_D M_R^{-1} M_D^T) U_\nu^* & 0 \\ 0 & U_N^T M_R U_N \end{bmatrix}. \tag{1.44}$$

In the above equation, the block elements are diagonalized by a 3×3 unitary matrix U_ν and a $n\times n$ unitary matrix U_N. Then, with the following definitions

$$\nu_{mL} \simeq U_\nu^\dagger(\nu_L - \varepsilon \nu_R^c),\ N_R \simeq U_N^\dagger(\nu_R + \varepsilon^T \nu_L^c), \tag{1.45}$$

$$m_\nu = U_\nu^\dagger (M_L^\dagger - \varepsilon M_D^T) U^*,\ M_N = U_N^T M_R U_N, \tag{1.46}$$

the diagonalized mass term can be written as

$$\begin{aligned} \mathcal{L}_{m_\nu} &= -\frac{1}{2}(\overline{\nu_{mL} + \nu_{mL}^c}) m_\nu (\nu_{mL} + \nu_{mL}^c) - \frac{1}{2}(\overline{N_R + N_R^c}) M_N (N_R + N_R^c) \\ &= -\frac{1}{2}\bar{\nu} m_\nu \nu - \frac{1}{2}\bar{N} M_N N, \end{aligned} \tag{1.47}$$

where

$$\nu \equiv \nu_{mL} + \nu_{mL}^c,\ N \equiv N_R + N_R^c \tag{1.48}$$

are Majorana neutrinos

$$\nu^c = \nu,\ N^c = N. \tag{1.49}$$

The matrix ε characterizes the mixing between heavy and light neutrinos and its elements can be estimated as

$$|\varepsilon_{ij}| \sim \sqrt{\frac{m_\nu}{m_N}}, \tag{1.50}$$

where m_ν is a mass of the order of the light neutrino masses and m_N is a mass of the order of the heavy neutrino masses. In most scenarios $|\varepsilon_{ij}|$ are very small then the three components of ν correspond to very light Majorana neutrinos and they are

mostly left-handed neutrinos ν_L, but n components of N will have very large masses and they are mostly right-handed neutrinos ν_R. This is known as standard (Type-I) see-saw mechanism [4, 20–24], and can explain the smallness of the neutrino masses.

New physics models generating the left-handed neutrino mass term at tree level with $M_L \sim v^2/M_{NP} \sim m_\nu$ in (1.37) through the effective operator in (1.38) can be categorized into three types [25] known as type-I, type-II and type-III [25–33]. Since there is only one dimension 5 operator (1.38) generating the left-handed neutrino mass term, all these heavy physics will give the same result.

A Lagrangian that can realize the type-I see-saw mechanism is

$$\mathcal{L} = \bar{N} i\not{\partial} N - \bar{\ell}\lambda\tilde{\phi}N - \frac{1}{2}\bar{N}^c M N + \text{H.c.}, \tag{1.51}$$

where N is a heavy fermion field with the following quantum numbers

$$(SU(3)\text{-charge},\ SU(2)\text{-isospin},\ U(1)\text{-hypercharge}) = (0, 0, 0), \tag{1.52}$$

and λ is a Yukawa coupling. After ϕ acquires VEV and the heavy fields are integrated out, we can obtain an effective Majorana mass term

$$\mathcal{L}_{\text{eff}} = -\bar{\tilde{\ell}}\phi(\lambda M^{-1}\lambda^T)^\dagger\tilde{\phi}^\dagger\ell + \text{H.c.} \tag{1.53}$$

$$\xrightarrow{\text{VEV}} -\overline{\nu_L^c} M_L \nu_L + \text{H.c.}, \tag{1.54}$$

where

$$M_L = \frac{v^2}{2}(\lambda M^{-1}\lambda^T)^\dagger. \tag{1.55}$$

When the scale of the heavy fermion masses becomes large the scale of neutrino masses become small. If the above Lagrangian has heavy fermion triplets instead of the singlets we will obtain the same result, which is the type-III.

The type-II see-saw mechanism can be realized by a Lagrangian

$$\mathcal{L} = \bar{\tilde{\ell}}\lambda\Phi_I\sigma^I\ell - \mu\tilde{\phi}^\dagger\Phi_I^*\sigma^I\phi + \text{H.c.} - 2M^2\Phi^\dagger\Phi, \tag{1.56}$$

where Φ is a heavy scalar field with quantum numbers $(0,1,1)$, σ^I are Pauli matrices, and μ is a dimensionful coefficient. $\Phi_I\sigma^I$ can be written in terms of charge eigenfield basis

$$\Phi_I\sigma^I = \begin{pmatrix} \Phi_3 & \Phi_1 - i\Phi_2 \\ \Phi_1 + i\Phi_2 & -\Phi_3 \end{pmatrix} = \begin{pmatrix} \Phi_+/\sqrt{2} & \Phi_{++} \\ \Phi_0 & -\Phi_+/\sqrt{2} \end{pmatrix}, \tag{1.57}$$

and $2\Phi^\dagger\Phi = |\Phi_0|^2 + |\Phi_+|^2 + |\Phi_{++}|^2$. The first term in the Lagrangian plus its Hermitian conjugate are Majorana mass terms, and the remaining terms correspond to a scalar potential. Through the minimization of the potential, Φ_0 will acquire a vacuum expectation value together with the scalar field of the Standard Model,

$$\phi_2 \xrightarrow{\text{VEV}} \frac{v}{\sqrt{2}},\ \Phi_0 \xrightarrow{\text{VEV}} \frac{v_\Phi}{\sqrt{2}},\ v_\Phi = \frac{\mu v^2}{\sqrt{2}M^2}. \tag{1.58}$$

If $M \sim \mu \gg v$ then the heavy scalars will be integrated out and neutrinos will acquire small Majorana masses proportional to v_Φ.

1.2.5 Right-handed neutrinos and leptogenesis

The heavy Majorana fermions, i.e., heavy Majorana neutrinos in (1.51) can decay into two modes

$$N \to e^- + \phi^+ \text{ or} \tag{1.59a}$$

$$N \to e^+ + \phi^-, \tag{1.59b}$$

where e is a charged lepton and $\phi^\pm$ are the first component of the scalar doublet in the Standard Model. The decay rates in the above two processes are different in general because the Yukawa coupling is a complex matrix. And the phases of the Yukawa coupling can not be removed by field redefinitions since the redefinitions are not canceled out in the Majorana mass term. Therefore we will have a non zero CP asymmetry

$$\epsilon_{\not{CP}} \equiv \frac{\Gamma(N \to e^- + \phi^+) - \Gamma(N \to e^+ + \phi^-)}{\Gamma(N \to e^- + \phi^+) + \Gamma(N \to e^+ + \phi^-)}. \tag{1.60}$$

This is the standard process of the leptogenesis and could contribute to the baryon asymmetry in the early universe because $B - L$ is conserved [34].

Chapter 2

Dimension five effective Lagrangian

If we include right-handed neutrinos in the collection of light fields in effective theory we may have new effective interactions involving ν_R. We will assume that there are two scales of new physics: the heavy Majorana mass M and Λ, and we will usually (but not always) assume $v < M < \Lambda$.

The electroweak part of the most general effective Lagrangian including ν_R up to dim-5 operators is

$$\mathcal{L}_{\text{eff}} = i\bar{\ell}\not{D}\ell + i\bar{e}_R\not{D}e_R - (\bar{\ell}Y_e e_R\phi + \text{H.c.}) + \cdots \tag{2.1a}$$

$$+ i\bar{\nu}_R\not{\partial}\nu_R - (\frac{1}{2}\overline{\nu_R^c}M\nu_R + \text{H.c.}) - (\bar{\ell}Y_\nu\nu_R\tilde{\phi} + \text{H.c.}) \tag{2.1b}$$

$$+ \overline{\nu_R^c}\zeta\sigma^{\mu\nu}\nu_R B_{\mu\nu} + (\bar{\tilde{\ell}}\phi)\chi(\tilde{\phi}^\dagger\ell) - (\phi^\dagger\phi)\overline{\nu_R^c}\xi\nu_R + \text{H.c.}, \tag{2.1c}$$

where ℓ is left-handed lepton doublet, e_R is right-handed charged lepton singlet, and ϕ is scalar doublet. Y_e and Y_ν are 3×3 and $3\times n$ complex matrices in flavor space respectively, where n is the number of flavors of ν_R. ζ is a $n\times n$ antisymmetric, χ is a 3×3 symmetric and ξ is a $n\times n$ symmetric complex matrix in flavor space respectively,

and all these couplings have energy dimension -1.

The first line (2.1a) of the above effective Lagrangian is the electroweak part of the Standard Model, the second line (2.1b) contains the operators of dimension 4 or less involving ν_R, and the third line has dim-5 effective operators. The second operator in the last line (2.1c), which was already introduced in the previous chapter, contributes to the left-handed Majorana-neutrino mass matrix M_L in (1.37) and provides the various lepton number violating interactions of left-handed neutrinos with Higgs. The first and the third operators in (2.1c) are new due to the addition of ν_R. The third operator in (2.1c) contributes to the right-handed Majorana-neutrino mass matrix M_R in (1.37) and generates lepton number violating interactions of right-handed neutrinos with Higgs.

The first operator in (2.1c), which has not been considered in the previous literature, produces unique electroweak magnetic couplings of ν_R. There are other types of effective operators producing neutrino magnetic moments: dim-6 or higher operators generating $\ell - \nu_R$ (Dirac-type) magnetic moments and dim-7 or higher operators generating $\ell - \ell$ (Majorana-type) magnetic moments, which are suppressed by their small couplings (that is, higher powers of $1/\Lambda$) compared to the dim-5 magnetic moments. In addition, these Dirac-type and Majorana type operators contribute to the light neutrino mass terms at the loop level, and therefore their couplings will be strongly constrained due to the small mass of light neutrinos. In Part 1, we will discuss the various effects of the dim-5 magnetic moment operator in collider experiments and astrophysical and cosmological processes.

2.1 New heavy physics for the dim-5 effective operators and coefficient estimates

We will present possible heavy physics models that can generate the dim-5 effective operators at low energies. From the heavy physics, we can identify the couplings of the effective operators in terms of the couplings and the masses of the heavy physics. More than one model of heavy physics can generate the same effective operator but they all give the same coefficient estimate in terms of the mass scale of the heavy physics as long as the effective operators are induced at the same level of diagram, i.e., tree or loop level. Therefore, we will consider only the simple heavy physics models for the coefficient estimations.

2.1.1 ν_L Majorana mass term $\bar{\ell}\phi\chi\tilde{\phi}^\dagger\ell$

As previously mentioned in Subsection 1.2.4, the new physics models generating the three types of see-saw mechanism can induce the ν_L Majorana mass term. For weakly coupled heavy physics, independent of the type of the see-saw mechanism, the coefficient estimate is

$$\chi \sim \frac{\lambda^2}{M_{\rm NP}}, \tag{2.2}$$

where λ is the coupling of the heavy particles to the Standard Model particles as we can see in Subsection 1.2.4, and $M_{\rm NP}$ is the mass of the corresponding heavy particle.

2.1.2 ν_R Majorana mass term $(\phi^\dagger\phi)\overline{\nu_R^c}\xi\nu_R$

This operator can be generated by either a heavy scalar $SU(2)$ singlet of hypercharge $Y = 0$ or a heavy fermion doublet of $Y = 1/2$. The coefficient estimate

is

$$\xi \sim \frac{\lambda^2}{M_{\rm NP}}, \tag{2.3}$$

where λ is the coupling of the heavy scalar particles to $\phi^\dagger\phi$ and $\nu\nu$ or the coupling of the heavy fermion to $\phi\nu$.

2.1.3 ν_R electroweak coupling $\overline{\nu_R^c}\zeta\sigma^{\mu\nu}\nu_R$

The ν_R magnetic moment operator cannot be generated at tree-level, but can be obtained from a one-loop diagram by a pair of scalar and fermion fields with opposite (nonzero) hypercharges or a pair of vector and fermion fields with opposite (nonzero) hypercharges. An example of the Lagrangian for the scalar-fermion pair is

$$\mathcal{L}_{\rm int} = \sum_i \lambda_i' \overline{\nu_{iR}^c} E\omega^* + \lambda_i \bar{E}\nu_{iR}\omega + \text{H.c.}, \tag{2.4}$$

where the subscript i is a flavor index, and we take λ_i and λ_j' are real. This Lagrangian generates the ν_R magnetic moment through the diagrams in figure 2.1 [35]. Then, the

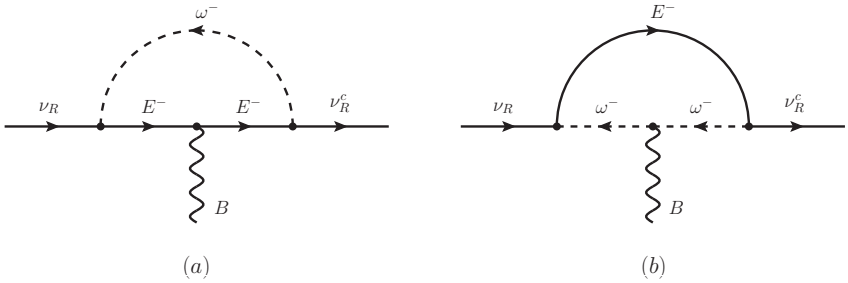

Figure 2.1: Diagrams generating $\overline{\nu_R^c}\zeta\sigma^{\mu\nu}\nu_R$.

coefficient estimate is

$$\zeta \sim \frac{g' y \lambda^2}{16\pi^2 M_E} \sim \frac{1}{16\pi^2 M_{\rm NP}}, \tag{2.5}$$

where we assumed $\lambda \sim \lambda'$ and $M_\omega \sim M_E$, g' is the coupling constant of $U(1)$ gauge boson in the covariant derivative of the Standard Model, and y is the hypercharge of E or ω.

The coupling is suppressed by $1/16\pi^2$ because of the loop. However, if the heavy physics is strongly coupled and right-handed neutrinos participate in these strong interactions then the coefficient can be estimated by naive dimensional analysis (NDA) [4, 36] as

$$\zeta \sim \frac{1}{M_{NP}}, \tag{2.6}$$

where $M_{\rm NP}$ is the scale of the strong interactions. This enhanced coupling may have interesting effects at colliders.

2.2 The effective Lagrangian in terms of mass eigenfields of Majorana neutrinos

After ϕ acquires a VEV, the effective Lagrangian (2.1) can be written in terms of the mass eigenfields of Majorana neutrinos. The mass terms have the same form as (1.37)

$$\mathcal{L}_{m_\nu} = -\bar{\nu}_L M_D \nu_R - \frac{1}{2}\overline{\nu_R^c} M_R \nu_R - \frac{1}{2}\overline{\nu_L^c} M_L \nu_L + \text{H.c.} \tag{2.7}$$

where the various mass matrices are defined in terms of the coupling constants as follows

$$M_R = M + \xi v^2,\ M_L = \chi v^2,\ M_D = Y_\nu \frac{v}{\sqrt{2}}. \tag{2.8}$$

From (1.45) and (1.48), we can have the expressions of the flavor eigenstates in terms of the Majorana mass eigenstates of neutrinos as follows

$$\nu_L \simeq P_L(U_\nu \nu + \varepsilon U_N^* N), \tag{2.9}$$

$$\nu_R \simeq P_R(U_N N - \varepsilon^T U_\nu^*), \tag{2.10}$$

where ε was defined and estimated in (1.43) and (1.50). P_L (P_R) is the left-handed (right-handed) projection operator for fermion fields and we have used the following

definitions

$$P_L \equiv \frac{1-\gamma^5}{2},\ P_R \equiv \frac{1+\gamma^5}{2}. \tag{2.11}$$

Plugging (2.9) and (2.10) into (2.1), each interaction terms will be written in terms of the mass eigenfields.

The ν_R magnetic moment term can be written as

$$\begin{aligned}\mathcal{O}_\zeta &\equiv \overline{\nu_R^c}\zeta\sigma^{\mu\nu}\nu_R B_{\mu\nu} + \text{H.c.} \\ &\simeq (\bar{N}U_N^T - \bar{\nu}U_\nu^\dagger\varepsilon)P_R\zeta\sigma^{\mu\nu}(U_N N - \varepsilon^T U_\nu^*\nu)(c_W F_{\mu\nu} - s_W Z_{\mu\nu}) + \text{H.c.},\end{aligned} \tag{2.12}$$

where $c_W \equiv \cos\theta_W,\ s_W \equiv \sin\theta_W$, θ_W is the weak mixing angle and we have used

$$B_\mu = c_W A_\mu - s_W Z_\mu^0, \tag{2.13}$$

here A_μ is the massless electromagnetic gauge boson and Z_μ^0 is the massive neutral electroweak gauge boson. As we can see from (2.12), $\mathcal{O}_\zeta$ produces six different electroweak interactions between the Majorana neutrinos and the neutral bosons. Let us summarize the new interactions schematically as follows

$$[N - N - (\gamma \text{ or } Z^0)] \times \zeta, \tag{2.14a}$$

$$[N - \nu - (\gamma \text{ or } Z^0)] \times \zeta\varepsilon, \tag{2.14b}$$

$$[\nu - \nu - (\gamma \text{ or } Z^0)] \times \zeta\varepsilon^2. \tag{2.14c}$$

The interactions are suppressed by ε or ε^2 depending on how many ν's get involved. The smallness of ε leads to a strong suppression of any electroweak-moment coupling to ν. Also, notice that since the electromagnetic moment coupling ζ is an antisymmetric flavor matrix, any two neutrinos in each of the above interactions must have two different flavors.

The ν_R mass term in terms of mass eigenfields will be

$$\begin{aligned}\mathcal{O}_{\nu_R} &\equiv -(\phi^\dagger\phi)\overline{\nu_R^c}\xi\nu_R + \text{H.c.} \\ &\simeq -\frac{(H+v)^2}{2}(\tilde{N}U_N^T - \bar{\nu}U_\nu^\dagger\varepsilon)P_R\xi(U_N N - \varepsilon^T U_\nu^*\nu) + \text{H.c.},\end{aligned} \tag{2.15}$$

where H is the Higgs boson. The new interactions are schematically as follows

$$[N - N - (H \text{ or } H^2)] \times \xi, \tag{2.16a}$$

$$[N - \nu - (H \text{ or } H^2)] \times \xi\varepsilon, \tag{2.16b}$$

$$[\nu - \nu - (H \text{ or } H^2)] \times \xi\varepsilon^2. \tag{2.16c}$$

$\mathcal{O}_{\nu_R}$ provides the interactions of Higgs bosons with Majorana neutrinos. The interactions involving ν are suppressed by ε or ε^2.

The ν_R Yukawa term can be written as

$$\begin{aligned}\mathcal{O}_{Y_\nu} &\equiv -\bar{\ell}\tilde{\phi}Y_\nu\nu_R + \text{H.c.} \\ &\simeq -\frac{1}{\sqrt{2}}(H+v)(\bar{\nu}U_\nu^\dagger + \bar{N}U_N^T\varepsilon^\dagger)P_R Y_\nu(U_N N - \varepsilon^T U_\nu^*\nu) + \text{H.c.},\end{aligned} \tag{2.17}$$

and the corresponding new interactions can be schematically shown as

$$[H - N - \nu] \times Y_\nu, \tag{2.18a}$$

$$[H - N - N] \times Y_\nu\varepsilon, \tag{2.18b}$$

$$[H - \nu - \nu] \times Y_\nu\varepsilon. \tag{2.18c}$$

$\mathcal{O}_{Y_\nu}$ also provides Higgs interactions with Majorana neutrinos, especially the dominant contribution to the decay of the lightest heavy neutrino into a Higgs boson and a light Majorana neutrino. For later uses, it is useful to see the relationship and the relative size of the neutrino Yukawa coupling Y_ν and the mixing matrix ε. From (1.43), (1.50) and (2.8)

$$Y_\nu = \sqrt{2}\frac{M_R}{v}\varepsilon, \;\; |Y_\nu| \sim \sqrt{2}\frac{m_N}{v}|\varepsilon|. \tag{2.19}$$

Finally, if we substitute (2.9) and (2.10) into the covariant derivative term of lepton doublet in (2.1a) and writing only the interaction terms

$$\begin{aligned} i\bar{\ell}\not{D}\ell &= \frac{g}{\sqrt{2}}W^-\bar{e}_L\gamma^\mu\nu_L + \text{H.c.} + \frac{g}{2c_W}Z^0_\mu\bar{\nu}_L\gamma^\mu\nu_L + \cdots \\ &\simeq \frac{g}{\sqrt{2}}W^-_\mu\bar{e}_L U^\dagger_e\gamma^\mu P_L(U_\nu\nu + \varepsilon U^*_N N) + \text{H.c.} \\ &+ \frac{g}{2c_W}Z^0_\mu(\bar{\nu}U^\dagger_\nu + \bar{N}U^T_N\varepsilon^\dagger)P_R\gamma^\mu(U_\nu\nu + \varepsilon U^*_N N) + \cdots . \end{aligned} \tag{2.20}$$

And the above equation can be expressed schematically

$$[W - \nu - e] \times g, \tag{2.21a}$$

$$[N - W - e] \times g\varepsilon, \tag{2.21b}$$

$$[Z^0 - \nu - \nu] \times g, \tag{2.21c}$$

$$[N - Z^0 - \nu] \times g\varepsilon, \tag{2.21d}$$

$$[Z^0 - N - N] \times g\varepsilon^2. \tag{2.21e}$$

Among the above interactions, (2.21b) and (2.21d) produce the decay of the lightest heavy Majorana neutrinos into a pair of Standard Model particles. If the heavy neutrinos are lighter than the W and Z, they would affect the decay modes of these particles, and LEP data can then be used to put a limit on ε.

Chapter 3

New interactions at colliders

From the fact that the heavy Majorana neutrinos have not been produced at LEP2 (Large Electron-Positron collider at 209 MeV) or Tevatron (proton-antiproton collider at 1 TeV), we can conclude that the heavy physics scale $M_{NP} > 100$ GeV. As it was mentioned in Subsection 2.1.3, if the heavy physics is weakly coupled, from (2.5) the coefficient will be suppressed as

$$\zeta \sim \frac{1}{16\pi^2 M_{NP}} \sim \frac{1}{15 \text{ TeV.}} \tag{3.1}$$

Therefore, we considered the case that the heavy physics is strongly coupled. We took

$$\zeta \sim \frac{1}{M_{\text{NP}}}, \tag{3.2}$$

and studied the interesting effects of ν_R magnetic moments on the observables at LEP, LHC and ILC (International Linear Collider).

3.1 Decay rates and decay lengths of heavy neutrinos

Since the Majorana particles are neutral, it is important to know their decay rates and lengths to detect them at colliders. In this section, the dominant decay modes

and lengths of the heavy neutrinos for relevant experiments will be discussed. For simplicity, we assumed $n = 2$, i.e., there are only N_1 and N_2 with $m_2 > m_1$.

If the ν_R magnetic moment coupling is strong enough to produce N_2 at a collider, it will decay dominantly by the same interaction as follows

$$N_2 \to N_1 + \gamma,$$
$$N_2 \to N_1 + Z^0, \tag{3.3}$$

unless m_1 and m_2 are almost the same, and if the second process is kinematically allowed. If N_2 is relatively heavy, $m_2 > 10$ GeV, the energy of the produced photon will be large then it could be a signal for N_2 decay. The decay length and the lifetime of N_2 is very short. For example, we found that if N_2 is produced at center of mass energy 100-1000 GeV then the decay length is well bellow 10^{-8} m unless $m_1 \simeq m_2$.

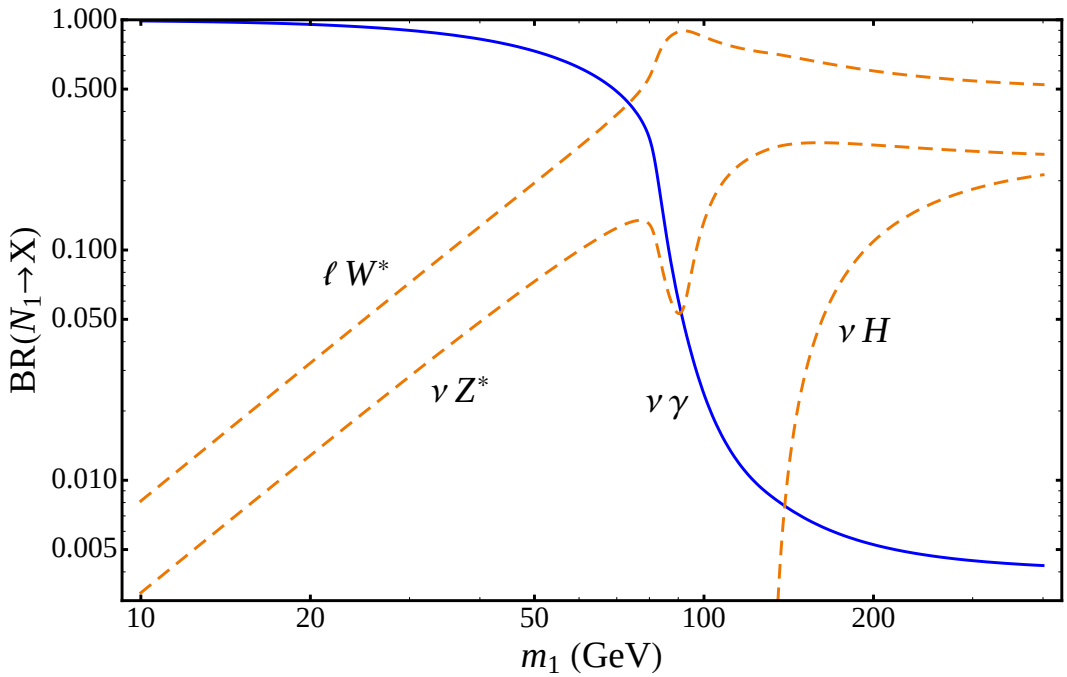

Figure 3.1: Decay branching ratio of N_1. Solid line for $N_1 \to \nu + \gamma$ and dashed line for $N_1 \to e + W* \to e+$ fermions, $N_1 \to \nu + Z^* \to \nu+$ fermions, and $N_1 \to \nu + H$ (see text). We take $\varepsilon \sim 10^{-6}$, $\Lambda_{\rm NP} = 10$ TeV and $m_H = 130$ GeV.

However the lightest heavy neutrino can only decay into Standard Model particles. As we can see from (2.14b), (2.21b) and (2.21d), the interactions are always suppressed by ε. In addition, (2.18a) generates the decay $H \to N + \nu$ and this process is also suppressed by ε, which we can see from the discussion below (A.8). Therefore the branching ratios of N_1 decay will be sensitive to the magnitude of ζ. The possible decay modes are as follows

$$N_1 \to \nu + \gamma, \tag{3.4a}$$

$$N_1 \to e + W^* \to e + \text{fermions}, \tag{3.4b}$$

$$N_1 \to \nu + Z^* \to \nu + \text{fermions}, \tag{3.4c}$$

$$N_1 \to e + W, \tag{3.4d}$$

$$N_1 \to \nu + Z^0, \tag{3.4e}$$

$$N_1 \to \nu + H, \tag{3.4f}$$

where the asterisk on top of W or Z means that the particle is a virtual because the mass of the decaying particle is not heavy enough to produce W or Z^0. Notice that (3.4b) and (3.4d) includes both cases of decaying into e^- and e^+. Fig. 3.1 shows an example of N_1 decay for $M_{\text{NP}} = 10$ TeV. In the figure, we can see that, for $m_1 < m_W$, (3.4a) dominates but as m_1 grows, (3.4b) and (3.4c) become more and more important.

For $m_1 > m_W$, the branching ratio of (3.4a) drops rapidly and (3.4d) becomes a dominant decay mode, and for $m_1 > m_Z$, (3.4e) becomes also important. For $m_1 > m_H$, N_1 can decay into ν and H. When $m_1 \gg m_H$, the decay ratios of (3.4e) and (3.4f) are equal and a half of (3.4d) (see the discussion below (A.8)). In figure 3.1 we assumed $M_{\text{NP}} = 10$ TeV but if $M_{\text{NP}} \sim 1$ TeV, then (3.4a) could be important even when $m_1 > m_W$. In figure 3.2 we estimated the decay lengths of a N_1 when the N_1 is

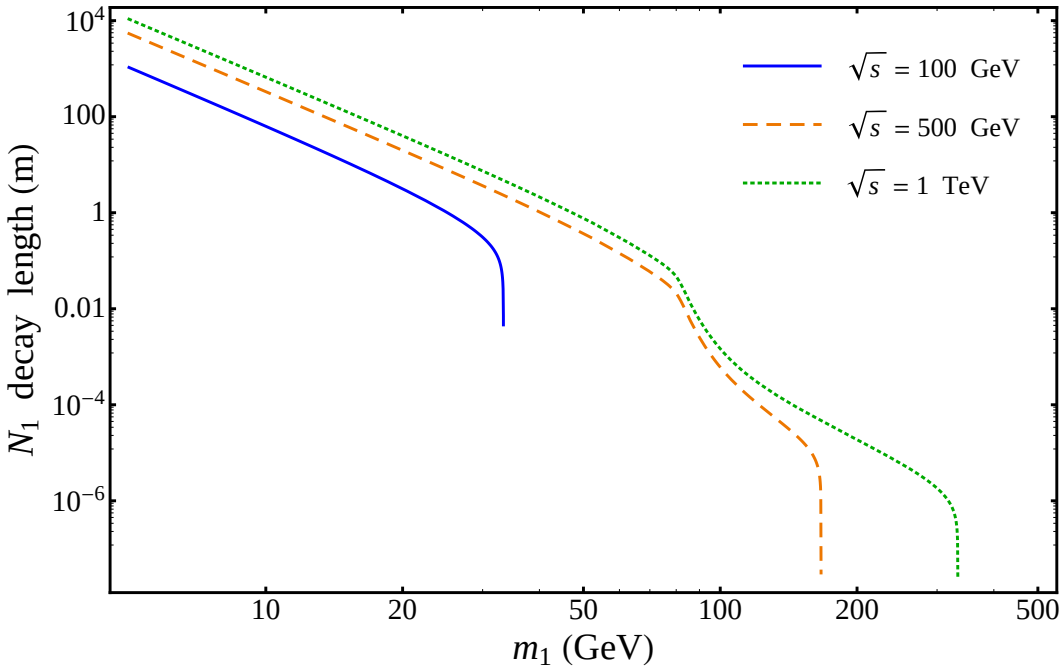

Figure 3.2: N_1 decay lengths for a N_1 produced together with a N_2 at CM. We present result for CM energies of $\sqrt{2} = 100$ GeV (solid line), 500 GeV (dashed line), and 1 TeV (dotted line); we took $m_2 = 2m_1, \Delta_{\rm NP} = 10$ TeV, and $\varepsilon = 10^{-6}$.

produced together with a N_2 by the ν_R magnetic moment interaction, for example, $e^- + e^+ \to N_1 + N_2$. The produced N_1 will decay into one of the possible modes in (3.4). We considered the case that the center of mass energies are 100 GeV, 500 GeV and 1 TeV. And we assumed $m_2 = 2m_1$, $\Lambda_{\rm NP} = 10$ TeV and $\varepsilon = 10^{-6}$. The figure shows that for $m_1 < 100$ GeV, the decay length is from a few millimeters to 10 km depending on the variables involved and the center of mass energy $\sqrt{s}$. In particular, for a certain range of m_2, N_2 could be observed through a displaced photon vertex [37–39].

3.2 Heavy Majorana neutrinos in electron-positron colliders

If N_1 and N_2 are sufficiently light, when they are produced at an electron-positron collider, their decay lengths could be long and will escape the detector. As we mentioned before, N_1 decay is suppressed by ε so the decay length could be very large. However, N_2 could decay into N_1 and an energetic photon. If the energy of the produced photon is large enough to be detected, then strong bounds on the magnetic moment coupling can be set, which depend on the masses of the heavy neutrinos. Notice that the results depend on the specific values of the masses and couplings, and we will not cover all possibilities in full detail, but will concentrate in cases where interesting effects might occur.

First, let us consider the case that Z^0 decays into N_1 and N_2 invisibly. We calculated the decay rate $\Gamma(Z^0 \to N_1 + N_2)$ by the ν_R magnetic moment coupling ζ and compared with the experimental data to obtain a bound on ζ. We assumed that only the standard decay modes $Z \to \nu_\ell + \bar{\nu}_\ell$ $(\ell = e, \mu, \tau)$ and $Z \to N_1 + N_2$ contribute to the invisible Z-decay. From the data at the LEP [40] we can have

$$\Gamma_{\text{inv}} = 3\Gamma_{\bar{\nu}\nu}^{\text{SM}} + \Gamma(Z^0 \to N_1 + N_2) = 499 \pm 1.5 \text{ MeV}. \tag{3.5}$$

Also from the decay rate of Z^0 into a pair of charged leptons [40]

$$\Gamma(Z \to \bar{\ell} + \ell) = 83.984 \pm 0.086 \text{ MeV}, \tag{3.6}$$

and the ratio of the neutrino and charged leptons partial widths calculated within the Standard Model

$$\frac{\Gamma_{\bar{\nu}\nu}^{\text{SM}}}{\Gamma_{\bar{\ell}\ell}^{\text{SM}}} = 1.991 \pm 0.001, \tag{3.7}$$

we find the mean value of $\Gamma(Z \to N_1 + N_2)$ as

$$\Gamma(Z \to N_1 + N_2) = \Gamma_{\rm inv} - 3\left(\frac{\Gamma_{\bar{\nu}\nu}}{\Gamma_{\bar{\ell}\ell}}\right)^{\rm SM}\Gamma_{\bar{\ell}\ell} \simeq -2.6 \pm 1.5 \text{ MeV}. \tag{3.8}$$

Since the mean value is negative, we use the Feldman and Cousins prescription [41] to obtain the following bound

$$\Gamma(Z^0 \to N_1 + N_2) < 0.48 \times 1.5 \text{ MeV} = 0.72 \text{ MeV} \quad 95\% \text{ C.L.}. \tag{3.9}$$

Comparing this value with the calculation (A.2), we obtain the bound on $|\zeta_{12}|$

$$M_{\rm NP} = \frac{1}{|\zeta_{12}|} > 7\sqrt{f_Z(m_Z, m_1, m_2)} \text{ TeV}, \tag{3.10}$$

where $f_Z(m_Z, m_1, m_2)$ is a phase space factor and defined in (A.1). For example, if $m_1 = m_2 = 35$ GeV then

$$M_{\rm NP} = \frac{1}{|\zeta_{12}|} > 1.9 \text{ TeV}. \tag{3.11}$$

Now we consider the case that ζ-coupling is large enough to produce N_1 and N_2 at the LEP. The dominant decay mode for N_2 is $N_2 \to N_1 + \gamma$ unless $m_1 \simeq m_2$. If the produced photon has energy $E_\gamma > 10$ GeV, it could be detected and separated from the background. The searches for this type of processes have been conducted at LEP1 [42–45] and at LEP2 [46–48]. If 5 GeV $< m_2 <$ 90 GeV and BR$(N_2 \to N_1 + \gamma) = 1$, one typically obtains upper bounds on the production branching ratio [42, 49]

$$\text{BR}(Z^0 \to N_1 + N_2) \sim 2 \times 10^{-6} - 8 \times 10^{-6}, \tag{3.12}$$

depending on m_1 and m_2. For example, if $m_1 = 0,\ 10 \text{ GeV} < m_2 < m_Z$ and if we use BR$(Z^0 \to N_1 + N_2) < 8 \times 10^{-6}$, we obtain

$$M_{\rm NP} = \frac{1}{|\zeta_{12}|} > 40 \text{ TeV}. \tag{3.13}$$

LEP2 data can also be used to obtain bounds on $|\zeta_{12}|$. For typical values of m_1 and m_2, one can obtain the upper bounds on the production cross section of the order of 0.1 pb for $\sqrt{s} = 207$ GeV. This means

$$M_{\rm NP} = \frac{1}{|\zeta_{12}|} > 1 \text{ TeV}. \tag{3.14}$$

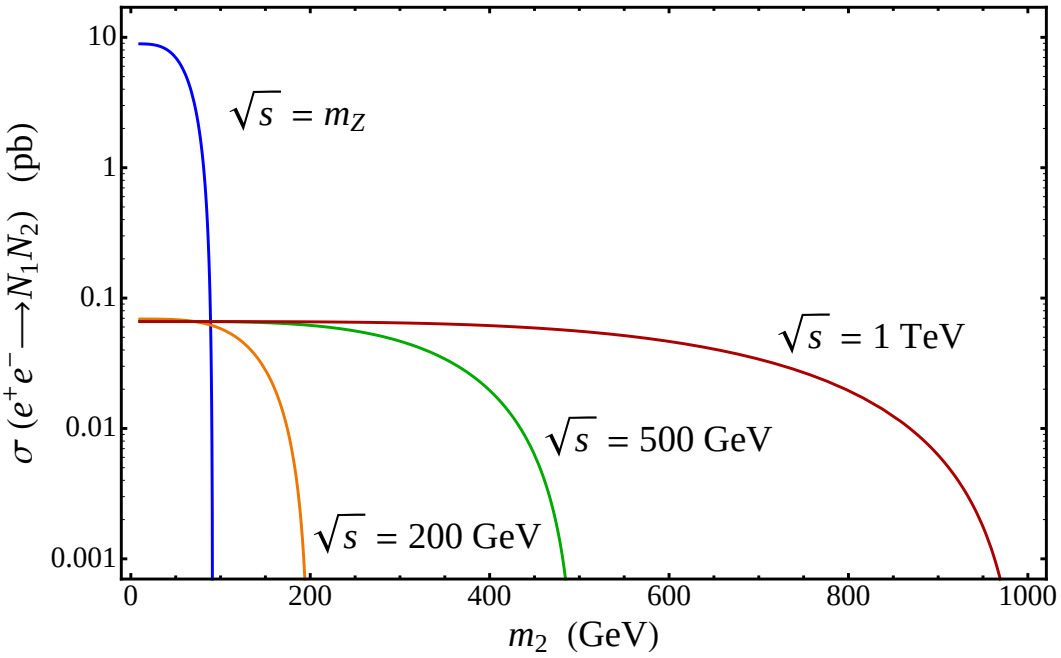

Figure 3.3: $e^+ + e^- \to N_1 + N_2$ as a fuction of the heavy neutrino mass, m_2, for different center of mass energies. We took $m_1 = 0, M_{\rm NP} = 10$ TeV

Figure 3.3 shows the cross section for $e^+ + e^- \to N_1 + N_2$ as a function of m_2 for four different $\sqrt{s}$ values. We took $m_1 = 0$ and $M_{\rm NP} = 10$ TeV. Here $\sqrt{s} = 200$ GeV is for LEP and $\sqrt{s} = 500$ GeV and $\sqrt{s} = 1$ TeV are for future electron-positron colliders, for example, the International Linear Collider (ILC). We can see from the figure that except for the collisions at $\sqrt{s} = m_Z$, cross sections are almost independent of the center of mass energy as long as the reactions are kinematically allowed.

3.3 Heavy Majorana neutrino production at the LHC

By the ν_R magnetic moment coupling, the heavy neutrinos can also be produced at hadron colliders through the Drell-Yan process. The differential cross section for proton-proton collisions can be calculated in terms of the partonic cross sections

$$d\sigma(p+p\to N_1+N_2+X)$$
$$=\sum_q\int_0^1 dx_1\int_0^1 dx_2\{f_q(x_1,\hat{s})f_{\bar{q}}(x_2,\hat{s})+(q\leftrightarrow\bar{q})\}d\hat{\sigma}(q+\bar{q}\to N_1+N_2,\hat{s}), \quad (3.15)$$

where $\hat{s}=x_1x_2s$ is the partonic center of mass invariant square mass, $\hat{\sigma}$ is the partonic cross section, and $f_q(x_1,\hat{s})$, $f_{\bar{q}}(x_2,\hat{s})$ are the parton distribution function for the proton. Using the partonic cross sections in (A.12) we can find the total cross section as a function of m_1, m_2 and ζ_{12}.

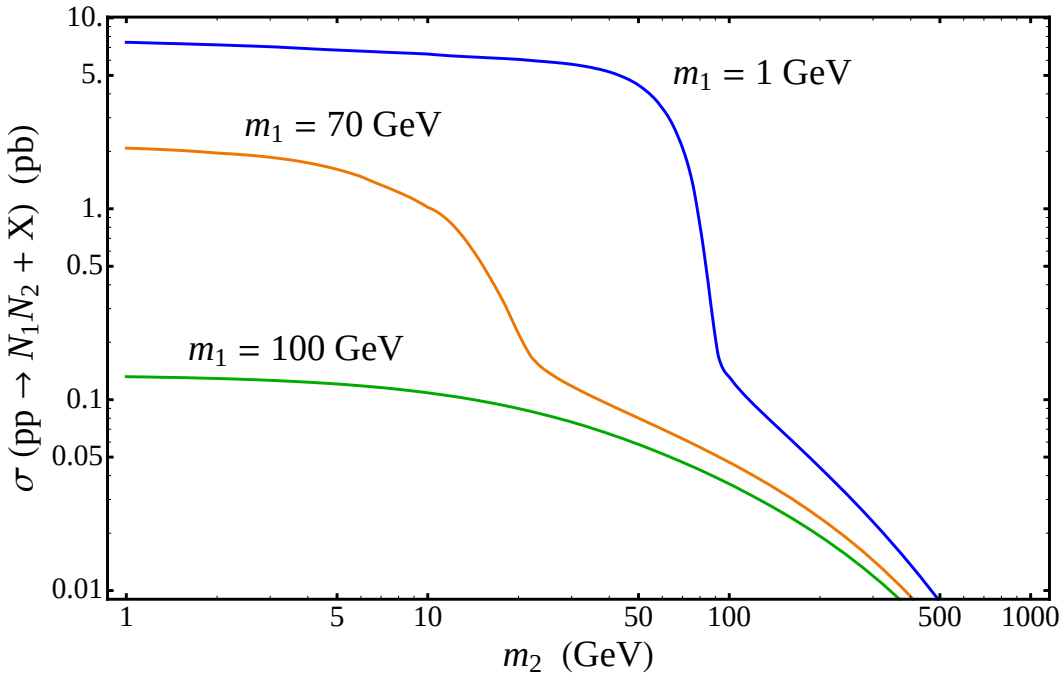

Figure 3.4: $p+p\to N_1+N_2$ cross section at the LHC ($\sqrt{s}=14$ TeV) as a functions of the mass of N_2. We took $M_{\rm NP}=10$ TeV and drew three curves for few representative masses of the N_1.

In figure 3.4, we show the total cross sections for the heavy neutrino production

at the LHC as a function of m_2 for three different m_1 examples. Here we assumed that $M_{\rm NP} = 10$ TeV and $\sqrt{s} = 14$ TeV. The cross sections are more than a 100 fb if $m_1 + m_2 < m_Z$. For larger m_2 the cross section decreases very fast.

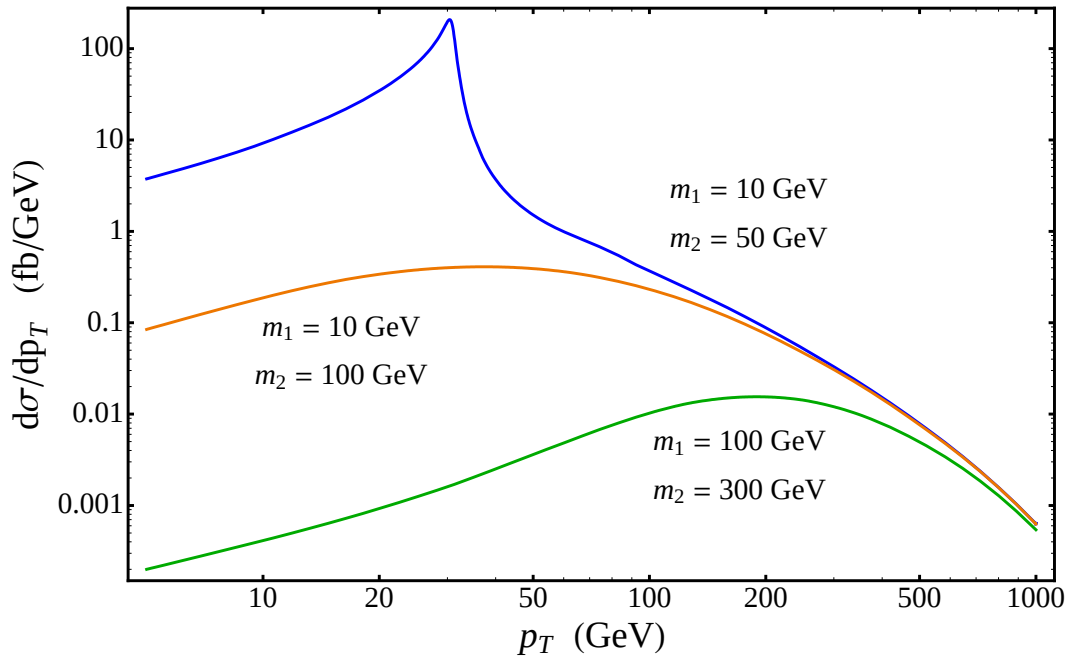

Figure 3.5: Transverse momentum distribution of the process $p + p \to N_1 + N_2 + X$ for different sets of heavy neutrino masses.

Figure 3.5 shows the differential cross section for $p + p \to N_1 + N_2 + X$ as a function of the transverse momentum p_T for different sets of m_1 and m_2. In the figure, we clearly see the peek of Z^0 boson for $m_1 + m_2 < m_Z$.

3.4 Higgs decays into heavy neutrinos

As mentioned in Section 2.2, ν_R mass term can generate Higgs decay into a pair of heavy neutrinos by the interaction (2.16a). The other two interactions which are suppressed by ε have been neglected. We also neglected the Yukawa interactions in (2.18), which are suppressed by Y_ν and ε. We computed the decay rate from (2.15),

which is given in (A.13), and compared this result with the Standard Model decay rates of the Higgs boson.

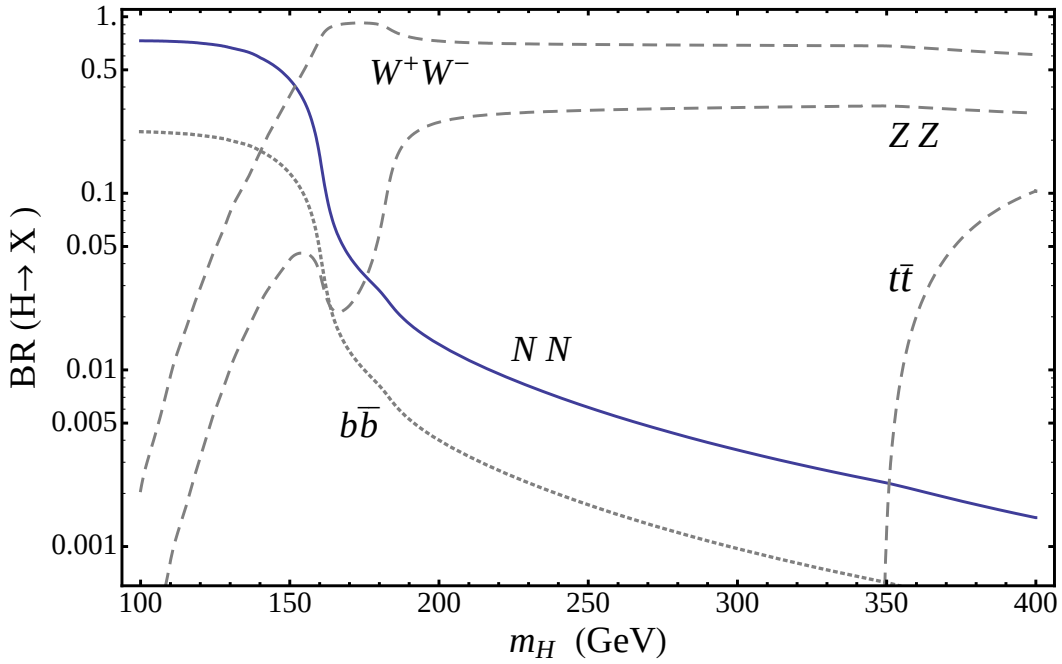

Figure 3.6: Estimated branching ratios for Higgs decays with the new-physics scale at $1/\xi = 10$ TeV. Heavy neutrino masses have been neglected.

In figure 3.6 we presented the branching ratio of the Higgs decay into pairs of heavy neutrinos and the Standard Model particles, where we assumed $M_{\mathrm{NP}\xi} = 10$ TeV and neglected the masses of the heavy neutrinos for simplicity. In the figure, we see that for $m_H < 2m_W$, the decay rate $\Gamma(H \to N_1 + N_2)$ is dominant. If the coupling $\xi = 1/M_{\mathrm{NP}\xi}$ becomes larger $\Gamma(H \to N_1 + N_2)$ could be dominant even for $m_H > 2m_W$. If the ν_R magnetic moment interaction takes place the produced N_2 can decay into N_1 and a photon which could be detected. Also N_1 can decay into a light neutrino and a photon. But this decay mode is suppressed by ε, therefore the decay length of the N_1 could be long and produce nonpointing photons which could be detected. If the ν_R magnetic moment coupling is weak or does not exist, there will be three-body decays

$N_1 \to W^* + \nu$ or $N_1 \to Z^* + \nu$ which are suppressed by ε.

Chapter 4

Astrophysical and cosmological effects

In this chapter we will consider the effects of the ν_R magnetic moment on several astrophysical and cosmological systems and processes. We will focus on some of the most interesting effects.

4.1 Astrophysical effects

Among the various astrophysical processes the cooling of red giant stars provides a very tight bound on the magnitude of the ν_R magnetic moment coupling ζ if the neutrinos involved in the process have sufficiently small masses. In the plasma of a red giant star a photon acquires a temperature-dependent effective mass. This massive photon is called a plasmon. The plasmon decays into a pair of neutrinos by ζ-coupling if the neutrinos are lighter than the plasmon. If the neutrinos are produced, they will leave the star and contribute to the cooling rate that is very sensitive to the size of the magnetic moment [50–56]. This provides an upper limit on the coupling.

From (2.12), the electromagnetic part of the electroweak moment coupling to the heavy neutrinos is

$$\mathcal{L}_{\rm EM} = c_W \bar{N}\sigma^{\mu\nu}(\zeta P_R + \zeta^\dagger P_L) N F_{\mu\nu}, \tag{4.1}$$

where we took $U_N = 1$. In a nonrelativistic nondegenerate plasma, the emissivity of neutrinos is dominated by transverse plasma [57], which have an effective mass equal to the plasma frequency ω_P. The decay rate of the plasmon into two heavy neutrinos are

$$\Gamma(\text{plasmon} \to N_i + N_j) = \frac{2c_W^2 |\zeta_{ij}|^2}{3\pi} \frac{\omega_p^4}{\omega} f_Z(\omega_P, m_i, m_j), \tag{4.2}$$

where i and j are the flavors of the heavy neutrinos, ω is the plasma energy in plasma rest frame, and f_Z is defined in (A.1). Then the total decay rate is

$$\begin{aligned} \Gamma(\text{plasmon} \to N + N) &= \frac{\mu_{\rm eff}^2}{24\pi} \frac{\omega_P^4}{\omega}, \\ \mu_{\rm eff}^2 &= 16 c_W^2 \sum_{\rm all} |\zeta_{ij}|^2 f_Z(\omega_P, m_i, m_j), \end{aligned} \tag{4.3}$$

where the sum runs over all allowed channels, $i > j$ such that $m_i + m_j < \omega_P$. Comparing (4.3) with the observation, we get [57]

$$\mu_{\rm eff} < 3 \times 10^{-12} \mu_\beta, \tag{4.4}$$

where μ_β is the Bohr magneton. This then provides a bound on $|\zeta_{ij}|$ when the heavy neutrinos are light

$$|\zeta_{ij}| < 8.5 \times 10^{-13} \mu_\beta; \quad m_{i,j} \ll \omega_P \simeq 8.6 \text{ KeV}, \tag{4.5}$$

which means

$$M_{{\rm NP}\zeta} > 4 \times 10^6 \text{ TeV}. \tag{4.6}$$

By the interactions (2.14b) and (2.14c), the plasmon can also decay into $N + \nu$ or $\nu + \nu$. But these processes are suppressed by ε and ε^2 respectively, and therefore they

can affect plasma decays only for extremely light N, $m_N \sim m_\nu$. In this case the masses of all the neutrinos can be neglected compared to the plasma frequency $\omega_P \sim 10$ KeV. However, if $m_N > \omega_P \sim 10$ KeV the plasma will decay into only light neutrinos. Since this interaction is suppressed by ε^2 the bounds from this process will be suppressed by ε^4, which is very small. For example, if $m_\nu = 0.1$ eV and $m_N = 10$ KeV then

$$M_{\rm NP} \gtrsim \left(\frac{m_\nu}{m_N}\right)^2 \times 4 \times 10^6 \text{ TeV} \sim 400 \text{ MeV}. \tag{4.7}$$

The discussion above can be applied to other astrophysical objects. The plasma frequency in the crust of a neutron star is $\omega_P = 1$ MeV. This larger frequency allow us to obtain bounds from processes involving heavier neutrinos. However, the much weaker limit [58],

$$\mu_{\rm eff} < 5 \times 10^{-7} \mu_\beta, \tag{4.8}$$

provides a weaker bound

$$M_{\rm NP} \gtrsim 23 \text{ TeV}, \quad m_{ij} \lesssim 1 \text{ MeV}. \tag{4.9}$$

This limit is interesting in the region 10 KeV $< m_N <$ 1 MeV, where red giant bounds do not apply. However, the bounds from neutron stars are less reliable than the bounds from red giant stars and supernovae.

The magnetic moment coupling also generates a new supernova cooling mechanism. In a supernova a light neutrino can transform to a heavy neutrino by the interaction (2.14b). The produced heavy neutrino will escape the star and contribute to the cooling rate. Since the process is suppressed by ε, with the observational limit $\mu_{\rm eff} < 3 \times 10^{-12} \mu_\beta$ [57] and $m_N < 30$ MeV (which is of the order of the maximum neutrino energy in the supernova core), we obtain a bound on the new physics scale

$$M_{\rm NP} \gtrsim 4 \times 10^6 \left(\frac{m_\nu}{m_N}\right) \text{ TeV}. \tag{4.10}$$

If $m_\nu \sim 0.1$ eV and $m_N = 10$ KeV then

$$M_{\rm NP} > 40 \text{ TeV}, \tag{4.11}$$

and for $m_\nu \sim 0.1$ eV and $m_N = 1$ MeV

$$M_{\rm NP} > 400 \text{ GeV}. \tag{4.12}$$

The bounds from the cooling of supernovae are weaker than the limit derived from neutron stars for 17 KeV $< m_N <$ 1 MeV.

It is also worth noting that if $m_N \sim 1$ KeV, N may contribute to the dark matter content of the universe [59–64].

4.2 CP asymmetries

Now let us consider an example of cosmological effect of the ν_R magnetic moment. The required conditions for any interactions to generate the baryon number asymmetry in the early universe are as follows [65]:

1. Baryon number (B) violation.

2. C and CP violation.

3. Departure from thermal equilibrium.

The ζ operator in (2.1c) violates lepton number by two and transforms under C and P as follows

$$\overline{\nu_R^c}\zeta\sigma^{\mu\nu}\nu_R B_{\mu\nu} + \text{H.c.} \xrightarrow{C} \overline{\nu_R^c}\zeta^*\sigma^{\mu\nu}\nu_R B_{\mu\nu} + \text{H.c.}, \tag{4.13}$$

$$\overline{\nu_R^c}\zeta\sigma^{\mu\nu}\nu_R B_{\mu\nu} + \text{H.c.} \xrightarrow{P} \overline{\nu_R^c}\zeta\sigma^{\mu\nu}\nu_R B_{\mu\nu} + \text{H.c.}, \tag{4.14}$$

where we used $\zeta^T = -\zeta$. Therefore the ν_R moment coupling satisfies the condition 1 (from the conservation of $B - L$) and 2. In a process in which the condition 3 is given, the electroweak moment may contribute to the baryogenesis in our universe [34].

As lepton-number-violating processes, we considered the standard decaying processes in (1.59)

$$N \to e^{\pm}\phi^{\mp}, \tag{4.15}$$

which receive a contribution from the ν_R magnetic moment in one-loop diagrams as in figure 4.1. The loop diagrams will generate a lepton asymmetry only if the decaying

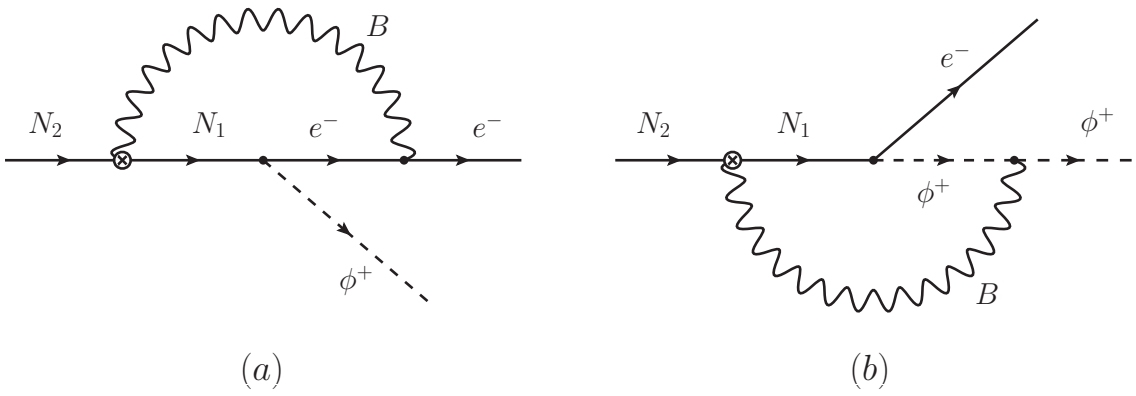

Figure 4.1: One-loop graphs involving electroweak moments contributing to lepton-number-violating heavy neutrino decays.

heavy neutrino is heavier than the virtual heavy neutrino in the loop. Because of this, this type of contribution may be relevant only when the lightest of the heavy neutrino states are degenerate or almost degenerate (for a recent review see [66]).

In the calculation of the decay rate of the heavy neutrinos, we assumed that $m_N \gg v$ so that all gauge bosons, leptons and scalars are massless except the heavy neutrino which has a mass by a Majorana mass term. We also neglected Yukawa couplings for charged leptons for simplicity. The relevant part of the Lagrangian in (2.1)

is

$$\mathcal{L}_N = \frac{i}{2}\bar{N}\partial\!\!\!/ N - \frac{1}{2}\bar{N}M_N N - \bar{\ell}Y_\nu P_R N\tilde{\phi} - \tilde{\phi}^\dagger \bar{N}Y_\nu^\dagger P_L \ell$$
$$+ \bar{N}\sigma^{\mu\nu}(\zeta P_R + \zeta^\dagger P_L)NB_{\mu\nu} - i\frac{g'}{2}(\partial_\mu\phi^\dagger)B^\mu\phi + i\frac{g'}{2}B^\mu\phi^\dagger(\partial_\mu\phi) \tag{4.16}$$

where M_N, without loss of generality, can be taken diagonal. Since we ignore Y_e in (2.1a), we can transform the lepton doublet ℓ by a unitary matrix so that Y_ν is Hermitian. But we do not have freedom to rotate ζ because of the Majorana mass term. For n flavors of N both Y_ν and ζ contain $n(n-1)/2$ phases. In particular, for $n = 3$ we will have a total of six phases. But even for $n = 2$ we will have two phases, which means, for simplicity, we can consider a case with $n = 2$ to have non zero CP asymmetries.

Assuming there are only two heavy neutrino flavors N_1 and N_2 with $m_2 > m_1$, we considered the following lepton-number-violating decays

$$N_2 \to e^- + \phi^+, \tag{4.17a}$$

$$N_2 \to e^+ + \phi^-, \tag{4.17b}$$

to calculate CP-violating asymmetry

$$\epsilon_{\not{CP}} \equiv \frac{\Gamma(N_2 \to e^- + \phi^+) - \Gamma(N_2 \to e^+ + \phi^-)}{\Gamma(N_2 \to e^- + \phi^+) + \Gamma(N_2 \to e^+ + \phi^-)}. \tag{4.18}$$

At tree level the amplitudes are simply

$$\mathcal{A}_0(N_2 \to e^-\phi^+) = Y_{e2}\bar{u}(p_e)P_R u(p_2), \tag{4.19}$$

$$\mathcal{A}_0(N_2 \to e^+\phi^-) = Y_{e2}\bar{v}(p_2)P_R v(P_e),$$
$$= -Y_{e2}^*\bar{u}(p_e)P_L u(p_2), \tag{4.20}$$

where Y_{ij} is an element of Y_ν, p_e and p_2 are the momenta of the outgoing electron and N_2 respectively, and we used $v(p) = u^c(p)$.

The one loop corrections to the decay processes involving the electroweak moment coupling ζ are given in figure 4.1. Since the ζ is antisymmetric the virtual heavy neutrino must be N_1. Therefore we can expect finite imaginary contributions from these diagrams. After a tedious calculation, we found the following finite CP-violating asymmetry in N_2 decays

$$\epsilon_{\not{CP}} = -\frac{g'}{2\pi}(m_2^2 - m_1^2)\frac{m_1}{m_2^3}\mathrm{Im}\left\{\frac{Y_{e2}Y_{e1}^*}{|Y_{e2}|^2}(\zeta_{12}^* m_2 + \zeta_{12} m_1)\right\}. \tag{4.21}$$

If $m_2 \gg m_1$ the above equation becomes

$$\epsilon_{\not{CP}} \simeq -\frac{g'}{2\pi} m_1 \mathrm{Im}\left\{\frac{Y_{e2}Y_{e1}^*}{|Y_{e2}|^2}\zeta_{12}^*\right\} \sim -\frac{g'}{2\pi}\frac{m_1}{\Lambda_{\mathrm{NP}}}\mathrm{Im}\left\{\frac{Y_{e2}Y_{e1}^*}{|Y_{e2}|^2}e^{-i\delta_{12}}\right\}, \tag{4.22}$$

where we have used $\zeta_{12} \sim e^{i\delta_{12}}/\Lambda_{\mathrm{NP}}$.

These contributions to CP violating asymmetry are relevant only for the decay of the heavier neutrinos and so could be relevant for leptogenesis only when m_1 and m_2 are relatively close [67–70]. In (4.21), if ζ_{12} is real, the CP asymmetry is maximum when

$$\frac{m_1}{m_2} = \frac{1+\sqrt{17}}{8} \simeq 0.64, \tag{4.23}$$

and the corresponding maximum CP asymmetry is

$$\epsilon_{\not{CP}} \simeq -0.97\frac{g'}{2\pi}\frac{m_1}{\Lambda_{\mathrm{NP}}}\mathrm{Im}\left\{\frac{Y_{e2}Y_{e1}^*}{|Y_{e2}|^2}\right\}. \tag{4.24}$$

For a comparison, we present the CP-asymmetry in the same decay processes in (4.15) by using the Lagrangian in (4.16) without the magnetic moment coupling. According to the reference [34] the CP asymmetry, from the interference of the tree diagram and the one-loop radiative correction by a Higgs boson, is

$$\epsilon_{\not{CP}} \sim \frac{9}{8\pi}\frac{m_1}{m_2}|Y_{22}|^2\delta, \tag{4.25}$$

where δ is the phase causing CP, Y is the Yukawa coupling matrix, and $m_{1,2}$ are heavy neutrino masses. In the calculation they assumed Y_{22} to be the largest element of Y and $m_2 \gg m_1$.

Chapter 5

Summary of Bounds, prospects and Conclusions of Part I

In Part 1, we have seen that the dimension five effective operators involving right-handed neutrinos open up observable effects in various interesting physical processes. The electroweak moment operator $\overline{\nu_R^c}\zeta\sigma^{\mu\nu}\nu_R B_{\mu\nu}$ + H.c. provides the richest phenomenology and the right-handed neutrino mass term $-(\phi^\dagger\phi)\overline{\nu_R^c}\xi\nu_R$ + H.c. can affect Higgs boson decays. After spontaneous symmetry breaking, the ξ operator gives rise to new interaction vertices involving right-handed neutrinos and the Higgs bosons as in (2.16). The vertex $H - N_i - N_j$ in (2.16a) provides new decay modes of the Higgs to heavy neutrinos if the processes are kinematically allowed. These new decay modes could dramatically change the Higgs decay branching ratios (see figure 3.6), especially in the region 100 GeV $< m_H <$ 160 GeV where the decaying into gauge bosons are kinematically not allowed. The new decays could result in an invisible Higgs, if the heavy neutrinos cannot be detected, or in new, enhanced detection channels if the right-handed neutrinos can be seen through their own decay channels, for example $N_2 \to N_1 + \gamma$ or

$N_1 \to \nu + \gamma$ and $N_1 \to e + W$ with a displaced vertex.

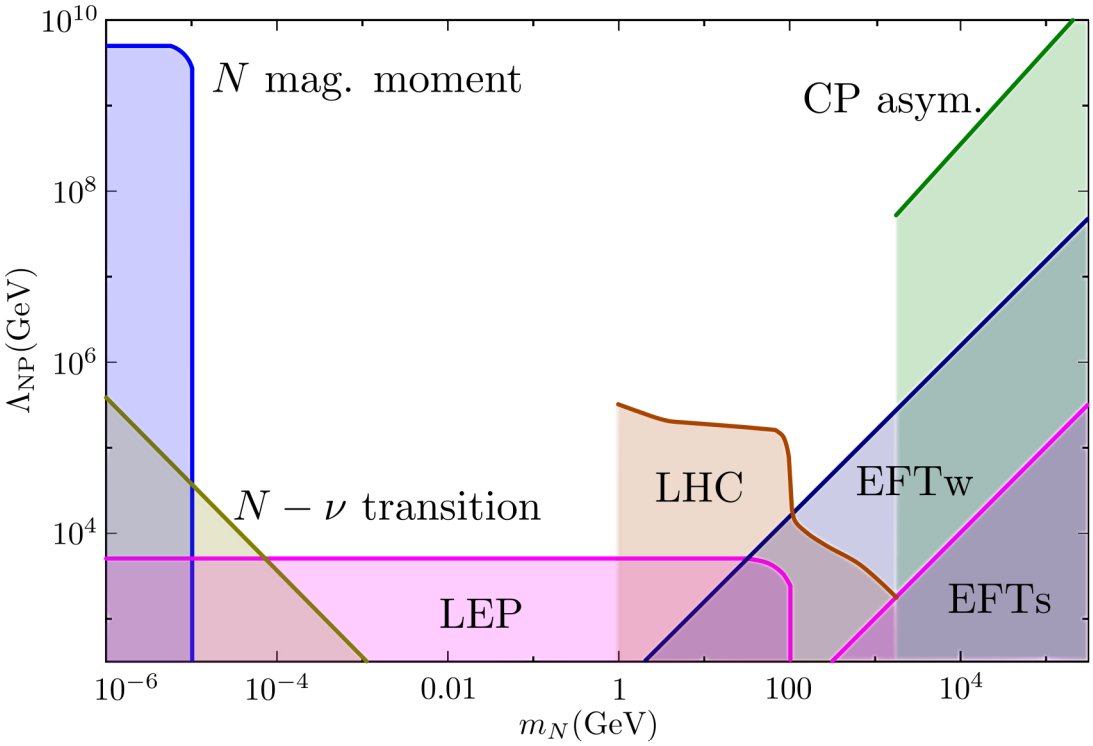

Figure 5.1: Summary of bounds and prospects. The shaded areas labeled N magnetic moment, $N-\nu$ transition, and LEP denote regions excluded by the corresponding observables; the areas marked EFTw and EFTs correspond to the regions where the EFT parametrization is inconsistent (for the weak- and strong-coupling regimes, respectively). Finally, shaded areas marked CP asym. and LHC denote the range of parameters where the dimension five electroweak moment might affect the corresponding observables. See the text for details.

In the basis of mass eigenfields, as shown in (2.14), the unique electroweak moment operator generates $N-N$, $N-\nu$, and $\nu-\nu$ magnetic moments, and $N-N$, $N-\nu$, and $\nu-\nu$ tensor coupling to the Z^0 bosons giving rise to a very rich phenomenology which depends basically on three parameters: the coupling matrix $\zeta \equiv 1/\Lambda_{\rm NP}$, the heavy-light mixing matrix ε, and the masses of the heavy neutrinos. Figure 5.1 summarizes the bounds of the ν_R magnetic moment coupling on the plane of the new physics scale and the heavy neutrino's mass. The figure also shows two interesting regions, the region relevant for the LHC and the region that can provide a relatively large CP asymmetry. In

the figure, except for the shaded area labeled as CP-asym, we assumed that $m_N = m_2$, $\varepsilon \sim \sqrt{m_\nu/m_N}$ with $m_\nu = 0.1$ eV and $m_1 = 0$. For the CP-asym area, we assumed $m_N = m_1 = 0.64 m_2$. Then we presented the regions in the $\Lambda_{\rm NP} - m_N$ plane forbidden by the red giant bound on the N magnetic moment, by the supernova bound on the transition magnetic moment $N - \nu$ and by the LEP bound from the invisible Z^0-boson decay width.

To test the new interactions involving heavy neutrinos at the LHC, one should produce first the heavy neutrinos and then one should detect them. The analysis of the detection is complicated and depends on the details of the spectrum and the capabilities of the detectors, but at least one should produce them with reasonable rate. In the shadowed area marked as LHC, the cross section of $p + p \to N_1 + N_2 + X$ is at least 100 fb.

The new interactions we have introduced new sources of CP violation which can modify the standard leptogenesis scenarios. In particular, we have found that the electroweak moment coupling gives additional contributions to the CP asymmetry in $N_2 \to e^- + \phi^+$ decay processes. These could be relevant in leptogenesis if $\epsilon_{\not{CP}} \sim (g'/2\pi)(m_N/\Lambda_{\rm NP}) > 10^{-6}$ and $m_N > 1$ TeV. This region is represented in figure 5.1 as the shaded area marked CP-asym.

Finally, in the regions marked as EFTw and EFTs, $m_N > M_{\rm NP}$ so the effective field theory is not available. In the region EFTw, $\Lambda_{\rm NP} = 16\pi^2 M_{\rm NP}$, and in the region EFTs, $\Lambda_{\rm NP} = M_{\rm NP}$.

From figure 5.1 we can draw the following conclusions:

(i) For $m_N \lesssim 10$ KeV, we obtain very tight bounds $\Lambda_{\rm NP} > 4 \times 10^6$ TeV coming from red giants cooling. This energy scale is too large that any effect of the electroweak

moment coupling would be totally negligible in any present or planned collider experiment. For $m_\nu \lesssim 1$ MeV, the cooling of neutron stars provides bounds $\Lambda_{\rm NP} \gtrsim 23$ TeV. Although, this limit is interesting in the region 10 KeV $\lesssim m_\nu \lesssim$ 1 MeV, where the red giant bounds do not apply, we did not put it in figure 5.1 because the bounds from neutron stars are less reliable than the bounds from red giants and supernovae.

(ii) For $m_N \lesssim 30$ MeV supernova cooling by the magnetic-moment-transitions $\gamma+\nu \to N$ provides bounds on the new physics scale. However, the amplitudes for these processes are suppressed by ε and therefore provide relatively weak bounds. For this mass range, the limits on the magnetic moment coupling from the cooling of red giants are obtained from plasmon decay into a pair of light neutrinos. However, these decay processes has amplitudes suppressed by ε^2 and therefore yields extremely weak constraints.

(iii) For $m_N \lesssim m_Z$, the invisible Z^0 decays impose $\Lambda_{\rm NP} \gtrsim 7 \times 10^3$ GeV, depending on the details of the heavy neutrino spectrum.

(iv) For $m_N \sim 1 - 200$ GeV and roughly 7 TeV $< \Lambda_{\rm NP} <$ 100 TeV, heavy neutrinos could be produced at the LHC with cross sections above 100 fb. Assuming there are three flavors of right-handed neutrinos, the heaviest two neutrinos would decay rapidly to hard photons which could be detected. The lightest heavy neutrino is quite long-lived and would produce nonpointing photons which could be detected.

In the above conclusions we have assumed that the new heavy physics generating the ν_R magnetic moment operator is strongly coupled, in which $1/\zeta = \Lambda = M_{\rm NP}$. If the operator is generated by perturbative physics it arises at one loop and one expects $\zeta \sim 1/(16\pi^2 M_{\rm NP})$. Thus, in this case, all the constraints discussed above still valid if

$\Lambda_{\rm NP}$ is replaced by $16\pi^2 M_{\rm NP}$. Then, if the new physics is weakly coupled, the interesting range for collider physics, $\Lambda_{\rm NP} \sim 10 - 100$ TeV, corresponds to $M_{\rm NP} \sim 0.1 - 1$ TeV, which is too low that the effective theory cannot be applied at LHC energies and one should use the complete theory generating the ν_R electroweak moments. Those complete theories should contain new particles carrying weak charges with masses $\sim 0.1 - 1$ TeV which should be produced in the LHC by the Drell-Yan process, for example.

There still remains much work to be done around this effective theory, especially concerning astrophysical and cosmological scenarios:

(a) The magnetic moment coupling may have effects in the early universe because it can potentially alter the equilibrium conditions of the heavy neutrinos and their decoupling temperature.

(b) Heavy neutrinos with masses $m_N \sim 1$ KeV could be a good dark matter candidate. The magnetic moment coupling could change significantly the analysis of this possibility.

(c) One should evaluate carefully the effects of the Majorana magnetic couplings on nonthermal leptogenesis.

(d) Sufficiently large ζ might lead to the trapping of the right-handed neutrinos in the supernova core.

Part II

New physics effects in neutrinoless double-beta decay

Chapter 6

Introduction

Neutrinoless double-beta decay ($0\nu\beta\beta$ decay) violates lepton number conservation which is valid in the Standard Model. $0\nu\beta\beta$ decay also requires neutrinos to be Majorana particles regardless of what model of new physics generated the decay. Observation of neutrinoless double beta decay will prove that there exist new physics beyond the Standard Model. In the following chapter, we will give a brief introduction to the $0\nu\beta\beta$ decay, the standard mechanism generating the decay, and current limit on the half life of the decay. In Chapter 7, we will list the Feynman diagrams and effective operators generating $0\nu\beta\beta$ decay, and discuss the possible types of new physics contributing to the effective operators. In Chapter 8, we will estimate the amplitude of the $0\nu\beta\beta$ decay for each effective operator from the Feynman diagrams and find the range of the new physics scale of each effective operator for the dominant contribution to the $0\nu\beta\beta$ decay over the contributions from other operators including the operator for the standard mechanism. Then we will estimate the lower limit of each new physics scale, and show that some types of heavy particles which can contribute to the $0\nu\beta\beta$ decay may be produced at the LHC. In addition, we will present the discovery limits on the

new physics scales for same-sigh dilepton production at the LHC.

6.1 Neutrinoless double-beta decay

In this section, a brief introduction to $0\nu\beta\beta$ decay will be given. The detailed reviews can be found in [71–73].

The $0\nu\beta\beta$ decay is a nuclear process emitting two electrons without anti-neutrinos

$$(A, Z) \to (A, Z + 2) + e^- + e^-, \tag{6.1}$$

where A and Z are the numbers of the nucleons and protons in the nucleus respectively. In this process two neutrons decay into two protons and two electrons, which violates lepton number by two. The standard mechanism generating the above process is diagrammatically shown in figure 6.1.

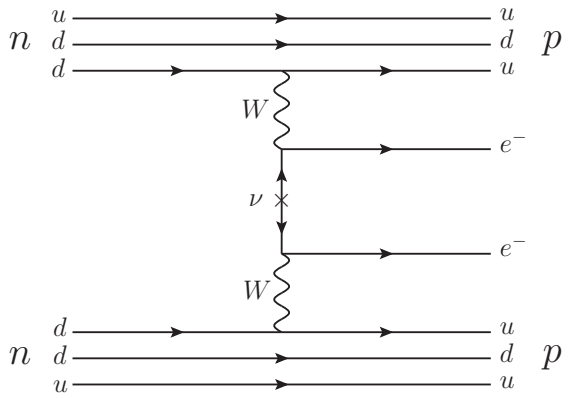

Figure 6.1: The standard mechanism for $0\nu\beta\beta$ decay. The cross mark indicates a Majorana mass insertion.

The amplitude of the standard mechanism in figure 6.1 is proportional to the hadron part times the weak interaction part. Since the average momentum of the exchanged virtual neutrino is typically 100 MeV which is well below the W mass, we

can use four-fermion effective vertex for the amplitude calculation

$$\mathcal{L}_{\text{weak}} = \frac{G_F}{\sqrt{2}} 2(\bar{e}_L \gamma^\mu \nu_{eL}) j_\mu, \tag{6.2}$$

where the Fermi constant G_F is

$$\frac{G_F}{\sqrt{2}} \equiv \frac{g^2}{8m_W^2} = \frac{1}{2v^2}, \tag{6.3}$$

and the charged hadronic current j_μ is

$$j_\mu \equiv 2\cos\theta_c \bar{u}_L \gamma_\mu d_L, \tag{6.4}$$

θ_c is the CKM angle. The lepton part of the decay amplitude is

$$(\bar{e}_L \gamma^\mu \overbrace{\nu_{eL})(\bar{e}_L \gamma_\mu}^{} \nu_{eL})^T = -\bar{e}_L \gamma^\mu \overbrace{\nu_{eL} \nu_{eL}^T}^{} C \gamma_\mu e_L^c, \tag{6.5}$$

where the contraction $\overbrace{\nu_{eL}\nu_{eL}^T}^{}$ is nonzero only if the neutrinos are Majorana particles. This means that if neutrinos are Majorana particles then the $0\nu\beta\beta$ decay can occur. However it has been shown that if the $0\nu\beta\beta$ decay occurs, the type of the neutrinos exchanged in the decay process have to be Majorana [74–76]. If the neutrinos have Majorana masses the contraction can be written in momentum space as

$$\overbrace{\nu_{eL}\nu_{eL}^T}^{} = \sum_k (U_{ek}^L)^2 P_L \frac{i(\not{q} + m_k)}{q^2 - m_k^2} P_L = \sum_k (U_{ek}^L)^2 m_k \frac{i}{q^2 - m_k^2} P_L, \tag{6.6}$$

where U_{ek}^L is the lepton mixing matrix, m_k is the mass of k-th Majorana neutrino, and q is the momentum of the virtual neutrino. Then the amplitude of $0\nu\beta\beta$ decay can be calculated as [71]

$$\mathcal{A}_{0\nu\beta\beta} = 2\left(\frac{G_F}{\sqrt{2}}\right)^2 \sum_k (U_{ek}^L)^2 m_k \bar{u}(p_1)\gamma^\mu P_L \gamma^\nu C \bar{u}^T(p_2) \tag{6.7}$$

$$\times \int d^4x_1 d^4x_2 e^{ip_1\cdot x_1 + ip_2 \cdot x_2} \int \frac{d^4q}{(2\pi)^4} \frac{ie^{-iq\cdot(x_1 - x_2)}}{q^2 - m_k^2} \tag{6.8}$$

$$\times \langle p' | T[J_\mu(x_1) J_\nu(x_2)] | p \rangle - (p_1 \rightleftarrows p_2), \tag{6.9}$$

where p_1 and p_2 are the momenta of the outgoing electrons, p and p' are the momenta of the initial and final nucleus respectively, and $J_\alpha(x)$ is the weak charged current in the Heisenberg representation. After applying the conventional approximations [77], and also using $m_\nu \ll |\vec{q}| \sim q_0$, one can find that the amplitude of the $0\nu\beta\beta$ decay is proportional to the effective Majorana-neutrino mass

$$\langle m_\nu \rangle = \sum_k (U^L_{ek})^2 m_k. \tag{6.10}$$

As we can see from the expression for the lepton mixing matrix (1.8), the effective mass depends on the Majorana-neutrino masses, mixing angles, CP-violating phases and Majorana phases.

6.2 Current limits in neutrinoless double-beta decay

What is measured in the experiment for $0\nu\beta\beta$ decay is the half life. The inverse half life, also called the decay rate, can be expressed as

$$\frac{1}{T^{0\nu}_{1/2}} = G(Z,Q)|M_{0\nu}|^2 |\langle m_\nu \rangle|^2, \tag{6.11}$$

where $G(Z,Q)$ is from the phase space integral, a function of the proton number Z, and the kinetic energy of the electrons $Q = M_i - M_f - 2m_e$, where M_i and M_f are the initial mass and final mass of the nucleus. $M_{0\nu}$ is the nuclear matrix element for the decay process.

Currently, the strongest limit on the half life is from the non-observation of $0\nu\beta\beta$ decay in Heidelberg-Moscow experiment [78]

$$T^{0\nu}_{1/2} > 1.9 \times 10^{25} \text{ years with } 90\% \text{ C.L.}, \tag{6.12}$$

which gives an upper limit of the effective Majorana-neutrino mass [78]

$$|\langle m_\nu \rangle| < 0.35 \text{ eV with } 90\% \text{ C.L.}. \tag{6.13}$$

At present, there are many planned future projects for the $0\nu\beta\beta$ decay experiment [79]. For example, GERDA experiment will test the effective Majorana-neutrino mass down to several 10 meV [80].

Notice that the above limits will be true only if the standard mechanism is the sole contribution to the $0\nu\beta\beta$ decay. If there are new mechanisms contributing to $0\nu\beta\beta$ decay, the limit on the effective Majorana-neutrino mass will be changed. In 2001 the subgroup of the Heidelberg-Moscow experiment claimed the observation of $0\nu\beta\beta$ decay [81–84] with the following half life and effective neutrino mass [84]

$$T_{1/2} = 2.23^{+0.44}_{-0.31} \times 10^{25} \text{ years}, \ |\langle m_\nu \rangle| = 0.32 \pm 0.03 \text{ eV}. \tag{6.14}$$

However, this observation does not have detailed analysis of systematic errors, and the only way to verify the claim is performing more sensitive experiment, for example, GERDA experiment [85].

Chapter 7

Diagrams and effective vertices

Since $0\nu\beta\beta$ decay is generated by non-standard physics (in the canonical case by Majorana masses) it is sensible to explore the types of new physics that can give rise to this effect. Since all the energies involved are well below the scale of new physics, the new physics effects can be catalogued using an effective Lagrangian. In this chapter, we list the relevant operators that can be separated into lepton-number-violating operators (LNVOs) and lepton-number-conserving operators (LNCOs). However, the LNCOs contribute only in the presence of right-handed neutrinos and in combination with a Majorana mass term.

Our goal is to determine the kinds of new physics that can affect $0\nu\beta\beta$ decay and to see what other observable effects they can have. The last point is important because one cannot differentiate between different contributions to $0\nu\beta\beta$ decay by doing this measurement only.

7.1 List of diagrams

Figure 7.1 shows all possible diagrams generating $0\nu\beta\beta$ decay produced by either LNVOs or LNCOs plus the Majorana mass insertion. We will use the same notation used in [86] for the diagrams by the LNVOs. For the diagrams by the LNCOs we will simply prime the notations for the diagrams by LNVOs. After the spontaneous symmetry breaking in the Standard Model, there can be one graph by a light Majorana neutrino mass term and five graphs by LNVOs. Also, we can have two graphs including both LNCO and the left-handed Majorana mass vertex.

7.2 List of contributing operators

In this section, we list the effective operators generating each effective vertex from D_ν to D_9 in figure (7.1). All the LNVOs up to dim-11, not containing gauge bosons were surveyed in [86] and [87]. We will use their notations for LNVOs. As mentioned in [87], we will omit the LNVOs which have the form of $(\phi^\dagger\phi) \times \mathcal{O}_{\Delta L=2}$ because the presence of those operators implies the presence of $\mathcal{O}_{\Delta L=2}$ and the contributions of those higher dimensional operators to the $0\nu\beta\beta$ decay is negligible compared to the contributions of the lower dimensional operators $\mathcal{O}_{\Delta L=2}$. For simplicity, we will not show the color indices of the fields in the effective operators but we will denote $SU(2)$ indices explicitly. Also note that the covariant derivative acting on a field in an operator can also act on the other fields in the operator, but mostly we will only show one example for each operator, and therefore the actual number of operators contributing to the $0\nu\beta\beta$ will be more than we present.

D_ν: Any operator generating left-handed Majorana neutrino mass term will

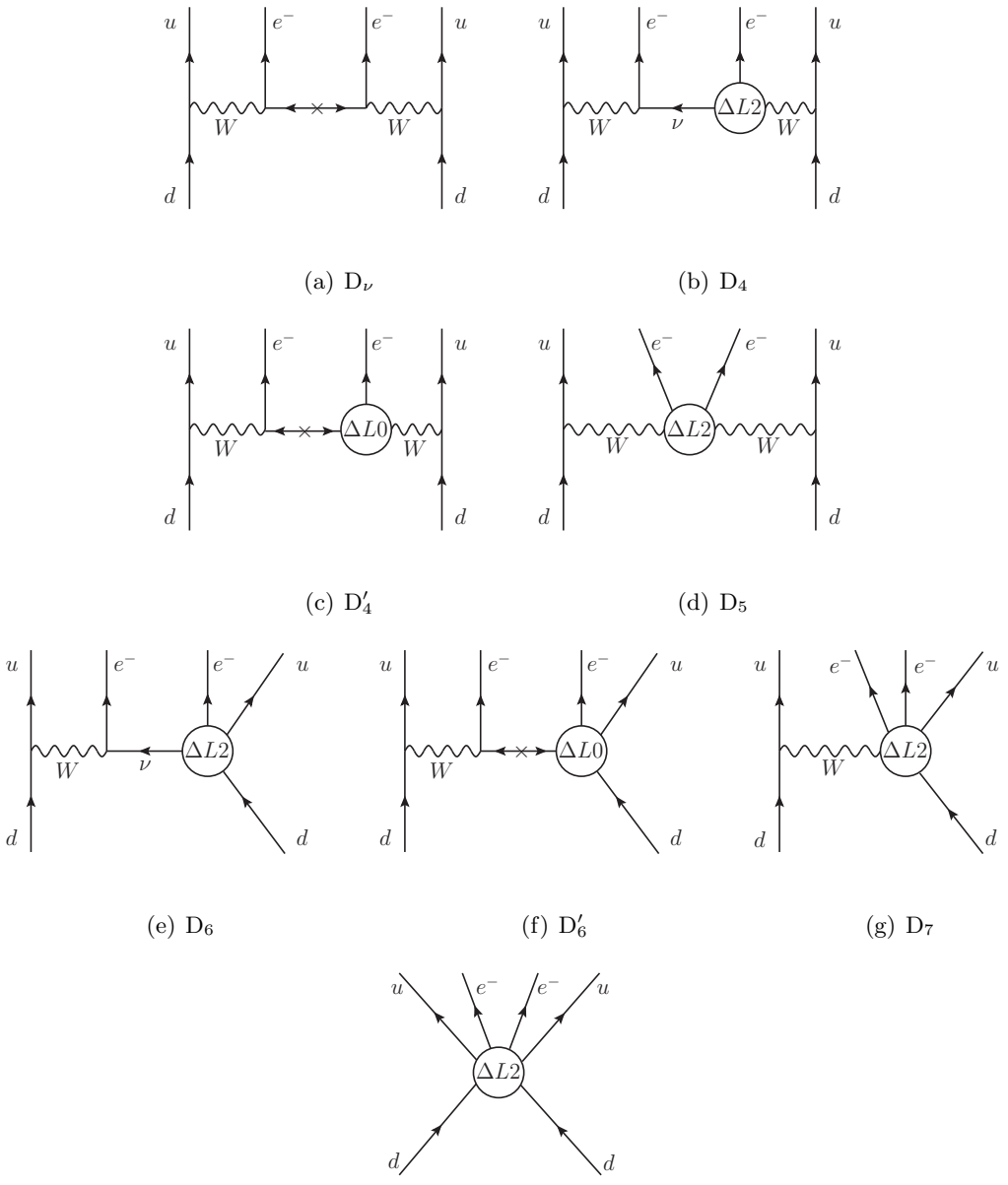

(a) D_ν (b) D_4

(c) D_4' (d) D_5

(e) D_6 (f) D_6' (g) D_7

(h) D_9

Figure 7.1: Graphs generating $0\nu\beta\beta$-decay. ν_L's are left-handed neutrinos and ν's are Majorana neutrinos.

contribute to D_ν. However, there is only one dim-5 LNVO contributing to the mass term at tree level, which is

$$\mathcal{O}_\nu = \bar{\bar{\ell}}\phi\chi\tilde{\phi}^\dagger\ell. \tag{7.1}$$

$\mathbf{D}_4$: There are three dim-7 LNVOs

$$\mathcal{O}_{g4a} = \bar{e}_R(\phi^\dagger i\not{D}\tilde{\phi})(\phi^\dagger\tilde{\ell}),$$
$$\mathcal{O}_{g4b} = (\bar{\ell}D_\mu\tilde{\ell})(\phi^\dagger D^\mu\tilde{\phi}),$$
$$\mathcal{O}_{g4c} = (\bar{\ell}\tilde{\phi})[(D_\mu\phi)^\dagger(D^\mu\tilde{\ell})]. \tag{7.2}$$

$\mathbf{D}'_4$: This graph includes both Majorana mass vertex and a LNCO. There are two dim-6 LNCOs contributing to D'_4

$$\mathcal{O}_{Ne\phi} = (\phi^T i\sigma^2 iD_\mu\phi)(\bar{\nu}_R\gamma^\mu e_R),$$
$$\mathcal{O}^{(3)}_{\phi\ell} = (\phi^\dagger iD_\mu\sigma^I\phi)(\bar{\ell}\gamma^\mu\sigma^I\ell), \tag{7.3}$$

where $\mathcal{O}_{Ne\phi}$ and $\mathcal{O}^{(3)}_{\phi\ell}$ were considered first in [88] and [89] respectively. However, the contributions of these operators are negligible when the corresponding new physics scales are less then $\sim$ TeV compared to other operators' contributions.

$\mathbf{D}_5$: There are two dim-7 LNVOs contributing to D_5

$$\mathcal{O}_{g5a} = [\overline{D_\mu\ell}\tilde{\ell}][(D^\mu\phi)^\dagger\tilde{\phi}],$$
$$\mathcal{O}_{g5b} = [\overline{D_\mu\ell}\tilde{\phi}][(D^\mu\phi)^\dagger\tilde{\ell}], \tag{7.4}$$

and one dim-9 LNVO

$$\mathcal{O}_{g5c} = \bar{e}_R e^c_R[\phi^\dagger(D_\mu\tilde{\phi})][\phi^\dagger(D^\mu\tilde{\phi})], \tag{7.5}$$

where $\tilde{\ell} \equiv i\sigma^2\ell^c$ and $\tilde{\phi} \equiv i\sigma^2\phi^*$. The above operators have not been studied in the previous literature.

$\mathbf{D}_6$: There are five dim-7 LNVOs and four of these operators can have Lorentz contractions by the antisymmetric tensors $\sigma_{\mu\nu} = \frac{i}{2}[\gamma^\mu, \gamma^\nu]$ instead of charge conjugation

C

$$\mathcal{O}_{3a} = (\bar{\ell}\tilde{\ell})(\bar{q}d_R\tilde{\phi}),\ \mathcal{O}'_{3a} = (\bar{\ell}\sigma_{\mu\nu}i\sigma^2\bar{\ell}^T)(\tilde{\phi}^T d_R^T\sigma^{\mu\nu}q^c),$$

$$\mathcal{O}_{3b} = (\bar{\ell}_i\ell_j^c)(\bar{q}_k\phi_\ell^* d_R)\epsilon_{ik}\epsilon_{j\ell},\ \mathcal{O}'_{3b} = (\bar{\ell}_i\sigma_{\mu\nu}\bar{\ell}_j{}^T)(d_R^T\sigma^{\mu\nu}\phi_\ell^\dagger q_k^c)\epsilon_{ik}\epsilon_{j\ell},$$

$$\mathcal{O}_{4a} = (\bar{\ell}_i\phi^\dagger\tilde{\ell})(\bar{u}_R q_i),\ \mathcal{O}'_{4a} = (\bar{\ell}_i\phi^\dagger i\sigma^2\sigma_{\mu\nu}\bar{\ell}^T)(q_i^T\sigma^{\mu\nu}u_R^c),$$

$$\mathcal{O}_{4b} = (\bar{\ell}\tilde{\ell})(\bar{u}_R\phi^\dagger q),\ \mathcal{O}'_{4b} = (\bar{\ell}i\sigma^2\sigma_{\mu\nu}\bar{\ell}^T)(q^T\sigma^{\mu\nu}\phi^* u_R^c),$$

$$\mathcal{O}_8 = (\bar{\ell}\tilde{\phi}\gamma_\mu e_R^c)(\bar{u}_R\gamma^\mu d_R), \tag{7.6}$$

and there are five dim-9 LNVOs

$$\mathcal{O}_5 = (\bar{\ell}\phi\phi^\dagger\tilde{\ell})(\overline{d_R^c}\phi^\dagger\tilde{q}),\ \mathcal{O}'_5 = (\bar{\ell}\phi\phi^\dagger i\sigma^2\sigma_{\mu\nu}\bar{\ell}^T)(d_R^T\sigma^{\mu\nu}\phi^\dagger\tilde{q}),$$

$$\mathcal{O}_6 = (\bar{\ell}\phi\phi^\dagger\tilde{\ell})(\bar{u}_R\phi^\dagger q),\ \mathcal{O}'_6 = (\bar{\ell}\phi\phi^\dagger i\sigma^2\sigma_{\mu\nu}\bar{\ell}^T)(q^T\sigma^{\mu\nu}\phi^* u_R^c),$$

$$\mathcal{O}_7 = (\bar{e}_R\gamma_\mu\phi^\dagger\tilde{\ell})(\bar{q}\tilde{\phi}\gamma^\mu\phi^\dagger q), \tag{7.7}$$

where the subscripts of the fields are $SU(2)$ indices and the repeated indices are assumed to be summed. The LNVOs in the above equation were introduced in [87] and [86].

$\mathbf{D}'_6$: This graph also contains both a Majorana mass vertex and a LNCO. There are three dim-6 LNCOs

$$\mathcal{O}_{\ell q}^{(3)} = (\bar{\ell}\gamma_\mu\sigma^I\ell)(\bar{q}\gamma^\mu\sigma^I q),$$

$$\mathcal{O}_{qde} = (\bar{\ell}e_R)(\bar{d}_R q),\ \mathcal{O}'_{qde} = (q^T\sigma_{\mu\nu}d_R^c)(e_R^T\sigma^{\mu\nu}\ell^c), \tag{7.8}$$

where the LNCOs were introduced in [89]. All these operators have negligible contributions to $0\nu\beta\beta$-decay.

$\mathbf{D}_7$: There is one dim-7 LNVO

$$\mathcal{O}_{g7a} = (\overline{iD_\mu\ell}\tilde{\ell})(\bar{u}_R\gamma^\mu d_R), \tag{7.9}$$

and the dim-9 LNVOs contributing to D_7 are

$$\begin{aligned}
\mathcal{O}_{g7b} &= (\bar{\ell} i D_\mu \tilde{\ell})(\bar{q}\gamma^\mu \tilde{\phi})(\phi^\dagger q), \\
\mathcal{O}_{g7c} &= \bar{\ell}_i(\phi^\dagger i D_\mu \tilde{\ell})\bar{q}_j\gamma^\mu(\phi^\dagger q)\epsilon_{ij}, \\
\mathcal{O}_{g7d} &= \bar{\ell}_i(\phi^\dagger i D_\mu \tilde{\ell})(\bar{q}\tilde{\phi})\gamma^\mu q_i, \\
\mathcal{O}_{g7e} &= (\bar{\ell}_i \ell_j^c)(\bar{q}_k\gamma^\mu q_j)(iD_\mu\phi)^\dagger\tilde{\phi}\epsilon_{ik}, \\
\mathcal{O}_{g7f} &= \bar{\ell}_i[(iD_\mu\phi)^\dagger\tilde{\ell}]\bar{q}_j\gamma^\mu(\phi^\dagger q)\epsilon_{ij}, \\
\mathcal{O}_{g7g} &= \bar{\ell}_i[(iD_\mu\phi)^\dagger\tilde{\ell}](\bar{q}\tilde{\phi})\gamma^\mu q_i, \\
\mathcal{O}_{g7h} &= (\bar{\ell}\gamma^\mu e_R^c)(iD_\mu\tilde{\phi})(\bar{q}d_R\tilde{\phi}), \\
\mathcal{O}_{g7i} &= (\bar{\ell}_i\gamma^\mu e_R^c)(\bar{q}_j d_R)[(iD_\mu\phi)^\dagger\tilde{\phi}]\epsilon_{ij}, \\
\mathcal{O}_{g7j} &= \bar{e}_R e_R^c(\bar{u}_R\gamma^\mu d_R)(\phi^\dagger i D_\mu\tilde{\phi}).
\end{aligned} \tag{7.10}$$

D_9: Only the LNVOs will contribute to D_9, which were listed in [86]. There are five dim-9 operators, $\mathcal{O}_{11b}$, $\mathcal{O}_{12a}$, $\mathcal{O}_{14b}$, $\mathcal{O}_{19}$, $\mathcal{O}_{20}$, and fifteen dim-11 operators, $\mathcal{O}_{24a}$, $\mathcal{O}_{28a}$, $\mathcal{O}_{28c}$, $\mathcal{O}_{32a}$, $\mathcal{O}_{36}$, $\mathcal{O}_{37}$, $\mathcal{O}_{38}$, $\mathcal{O}_{47a}$, $\mathcal{O}_{47d}$, $\mathcal{O}_{53}$, $\mathcal{O}_{54a}$, $\mathcal{O}_{54d}$, $\mathcal{O}_{55a}$, $\mathcal{O}_{59}$, $\mathcal{O}_{60}$.

7.3 Possible types of new physics contributing to each operator

Each effective operator can be induced by one or more models of new physics. Since the form of an effective operator is independent of the type of new physics, we will mostly consider simple examples of heavy physics except for the operators generating D_5. To denote the heavy fields, we will use the following notations:

$$\Phi = \text{scalar},\ \Psi = \text{fermion},\ X = \text{vector}, \tag{7.11}$$

and their quantum numbers will be indicated as

$$(I, Y) = (SU(2)\text{-isospin}, U(1)\text{-hypercharge}) \tag{7.12}$$

or in the graph, the quantum numbers will be appeared as subscripts, for example, $\Phi_{I,Y}$.

Notice that the diagrams in this section will simply list the minimal set of heavy fields that the new physics must contain in order to generate a given operator. In general a complete model of the heavy physics will contain additional fields and interactions, these do not contribute to the operators being studied, but can have other low-energy effects. This can have the advantage that a complete model can have many more predictions, but it is also possible that the current experimental constraints on the other effects are so strong as to insure that the contribution to $0\nu\beta\beta$ is negligible.

D$_\nu$: As we mentioned in the introduction of Part 1, the operator $\mathcal{O}_\nu$ can be generated though the see-saw mechanisms by the following heavy particles

$$\Psi_{0,0},\ \Psi_{1,0},\ \Phi_{1,1}. \tag{7.13}$$

D$_4$: $\mathcal{O}_{g4}$ can be induced at tree level from a new physics. The Lagrangian is

$$\begin{aligned}\mathcal{L}_{\mathcal{O}_{g4}} &= \bar{\Psi} i \not{D} \Psi - M_\Psi \bar{\Psi}\Psi - M_\Phi^2 \Phi^\dagger \Phi \\ &\quad + (Y \bar{\ell} \sigma^I \Psi_I \tilde{\phi} + Y' \bar{\Psi}_I \Phi_I^* e_R^c + v_\Phi \phi^+ \sigma^I \Phi_I \tilde{\phi} + \text{H.c.}),\end{aligned} \tag{7.14}$$

where $\Psi = (1, 0)$ and $\Phi = (1, 1)$. Y's are coupling constants, v_Φ is a massive coupling constant of the order of M_Φ for consistency, and the corresponding interaction is showed in figure 7.2. However, both Ψ and Φ can also generate $\mathcal{O}_\nu$ at tree level and induce the interaction D$_\nu$. This means that the physics scale Λ_{g4} is the same as Λ_ν and constrained through both diagrams D$_\nu$ and D$_4$ from $0\nu\beta\beta$ decay but the contribution of the heavy physics through the diagram D$_4$ is negligible compared to the contribution through D$_\nu$.

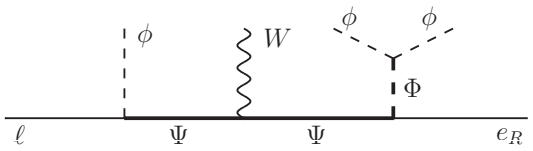

Figure 7.2: A new physics diagram generating $\mathcal{O}_{g4}$ (D_4). This diagram involves heavy physics contributing to D_ν at tree level. $\Psi = (1,0),\ \Phi = (1,1)$.

The exception is the heavy physics in figure 7.3 [90]. This heavy physics induces D_4 but does not induce D_ν at tree level. In the figure, the heavy vector X has quantum numbers $(\frac{1}{2}, \frac{3}{2})$ and X' has quantum numbers $(0,1)$ or $(1,1)$.

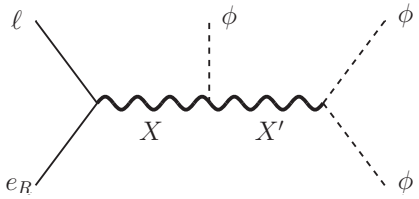

Figure 7.3: A new physics that contributes to D_4 but does not contribute to D_ν at tree level. $X = (\frac{1}{2}, \frac{3}{2}),\ X' = (0,1)$ or $(1,1)$.

$\mathbf{D}'_4$: $\mathcal{O}_{Ne\phi}$ can be generated from the following Lagrangian

$$\mathcal{L}_{\mathcal{O}_{Ne\phi}} = i\bar{\Psi}\not{D}\Psi - M_\Psi\bar{\Psi}\Psi + (Y\overline{\nu_R^c}\phi^\dagger\Psi + Y'\bar{\Psi}\tilde{\phi}e_R^c + \text{H.c.}), \tag{7.15}$$

where $\Psi = (\frac{1}{2}, \frac{1}{2})$, and Y and Y' are coupling constants. The corresponding interaction is in figure 7.4.

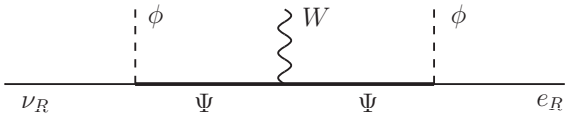

Figure 7.4: A new physics diagram inducing $\mathcal{O}_{Ne\phi}$ (D'_4), $\Psi = (\frac{1}{2}, \frac{1}{2})$.

$\mathcal{O}^{(3)}_{\phi\ell}$ can be generated from following Lagrangian

$$\mathcal{L}_{\mathcal{O}^{(3)}_{\phi\ell}} = \bar{\Psi} i \not{D} \Psi - M_\Psi \bar{\Psi}\Psi + (Y \bar{\ell} \Psi_I \sigma^I \tilde{\phi} + Y' \tilde{\phi}^\dagger \sigma^I \bar{\Psi}_I \ell + \text{H.c.}), \tag{7.16}$$

where $\Psi = (1, 0)$, and the corresponding interaction is in figure 7.5.

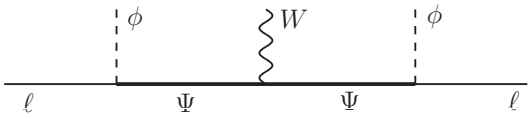

Figure 7.5: A new physics inducing $\mathcal{O}^{(3)}_{\phi\ell}$ (D'_4). $\Psi = (1, 0)$.

$\mathbf{D}_5$: Dim-7 $\mathcal{O}_{g5a,b}$ can be obtained from the following Lagrangians

$$\mathcal{L}_{\mathcal{O}_{g^5}} = \bar{\Psi} i \not{D} \Psi - M_\Psi \bar{\Psi}\Psi + (Y \bar{\ell} \sigma^I \Psi_I \tilde{\phi} + Y' \phi^\dagger \bar{\Psi}_I \sigma^I \tilde{\ell} + \text{H.c.}), \tag{7.17}$$

$$\mathcal{L}'_{\mathcal{O}_{g^5}} = (D_\mu \Phi)^\dagger (D^\mu \Phi) - M^2_\Phi \Phi^\dagger \Phi + (v_\Phi \phi^\dagger \Phi_I \sigma^I \tilde{\phi} + Y_\Phi \bar{\ell} \Phi^*_I \sigma^I \tilde{\ell} + \text{H.c.}), \tag{7.18}$$

where $\Psi = (1, 0)$ and $\Phi = (1, 1)$. The corresponding interactions are in figure 7.6. These

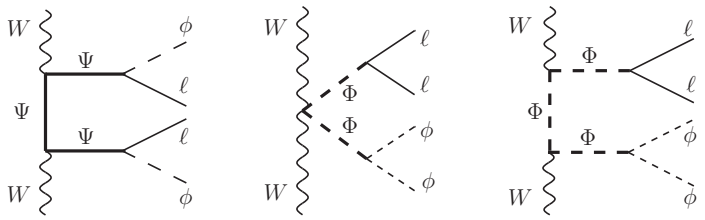

(a) (b) (c)

Figure 7.6: New physics diagrams generating $\mathcal{O}_{g5}$ (D_5). All these diagrams involve heavy physics contributing to D_ν. $\Psi = (1, 0)$, $\Phi = (1, 1)$.

heavy particles can also generate $\mathcal{O}_\nu$.

Dim-9 $\mathcal{O}_{g5c}$ can be induced by the same heavy particles generating $\mathcal{O}_\nu$, but there are also heavy physics models inducing $\mathcal{O}_{g5c}$ but not $\mathcal{O}_\nu$. The heavy physics and their particles are presented in figure 7.7.

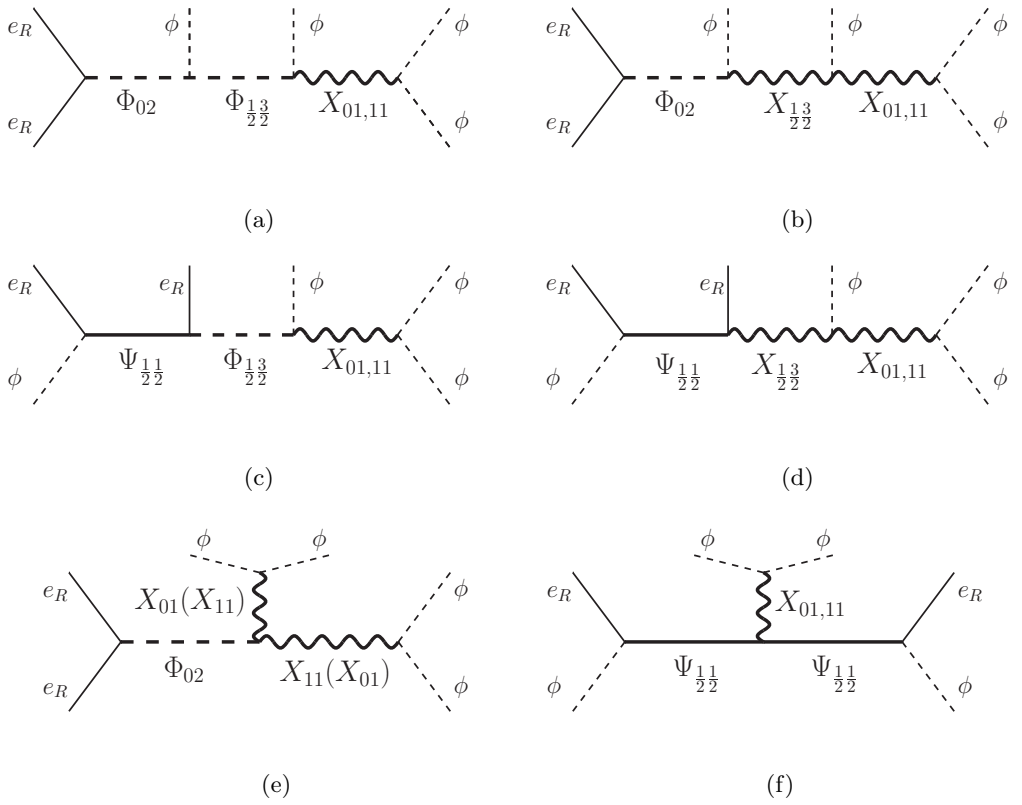

Figure 7.7: New physics diagrams generating dim-9 $\mathcal{O}_{g5c}$ (D_5). Subscripts of the fields denote isospin and hypercharge, for example, Φ_{IY} denotes a heavy scalar with isospin I and hypercgarge Y.

$\mathbf{D}_6$: $\mathcal{O}_{3a}$ can be obtained from the following Lagrangian

$$\mathcal{L}_{\mathcal{O}_{3a}} = (D_\mu \Phi)^\dagger (D^\mu \Phi) + (D_\mu \Phi')^\dagger (D^\mu \Phi') - M_\Phi^2 |\Phi|^2 - M_{\Phi'}^2 \Phi'^\dagger \Phi'$$
$$+ Y_\Phi \bar{\ell} \tilde{\ell} \Phi^* + Y_{\Phi'} \bar{q} \Phi' d_R + v_\Phi \Phi'^\dagger \tilde{\phi} \Phi + \text{H.c.}, \tag{7.19}$$

where $\Phi = (0, 1)$ and $\Phi' = (\frac{1}{2}, \frac{1}{2})$. The corresponding interaction is in figure 7.8.

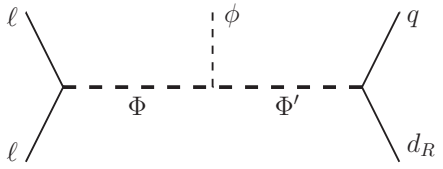

Figure 7.8: A new physics diagram generating $\mathcal{O}_{3a}$ (D_6). $\Phi = (0, 1)$, $\Phi' = (\frac{1}{2}, \frac{1}{2})$.

D_6': $\mathcal{O}_{\ell q}^{(3)}$ can be induced from a Lagrangian

$$\mathcal{L}_{\mathcal{O}_{\ell q}^{(3)}} = -\frac{1}{4}F_{\mu\nu}F^{\mu\nu} + Y\bar{\ell}\gamma^{\mu}X_{\mu}^{I}\sigma^{I}\ell + Y'\bar{q}\gamma^{\mu}X_{\mu}^{I}\sigma^{I}q, \tag{7.20}$$

where $X = (1, 0)$ and the corresponding interaction is in figure 7.9.

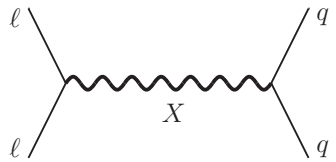

Figure 7.9: A new physics diagram generating $\mathcal{O}_{\ell q}^{(3)}$ (D_6'). $X = (1, 0)$.

D_7: $\mathcal{O}_{g7a}$ has both SU(2)-singlet and doublet fermions without ϕ's, and therefore, it can be generated only at the loop-level.

The heavy physics models generating the operators contributing to D_9 are listed in [87]. The new physics diagrams in this section give possible cases generating a given operator. Although there is no guarantee that a complete model that contains these particles will satisfy all experimental constraints, it still has a measurable effect at a current or near future experiment.

Chapter 8

Estimates and calculations

We will estimate the amplitudes of the $0\nu\beta\beta$ decay by using the diagrams in figure 7.1 for different effective operators, and evaluate the decay rate explicitly for $\mathcal{O}_{g5}$. The amplitude for the $0\nu\beta\beta$ decay is proportional to the multiplication of the weak interaction part (the amplitude for a graph in figure 7.1) and the strong interaction part which is incorporated in the nuclear matrix element. The calculation of the nuclear matrix elements is complicated many body nuclear physics problem. However, we will assume that the strong interaction part of the decay amplitude for each effective operator is in the same order of magnitude, and therefore we will concentrate on the weak interaction part of the amplitude. Then, based on the amplitude estimates, we will evaluate the ranges of the new physics scales for the dominant contributions to the $0\nu\beta\beta$ decay, and obtain the limits on the new physics scales for each diagram by using the data from currently the most sensitive $0\nu\beta\beta$ decay experiment. In addition, we will present the discovery limits on the new physics scales for same-sigh dilepton production at the LHC.

8.1 The amplitude estimate for each case

In this section, we will present amplitude estimates for different effective vertices. From the diagrams in figure 7.1, amplitudes can be estimated by using the following rules:

(i) For each Standard Model W vertex, include a factor of g

(ii) Replace each W propagator by $1/(g^2v^2)$

(iii) Replace each ν_L propagator by $1/Q$

(iv) Replace each contraction of ν_L and ν_L^T by m_ν/Q^2

(v) Replace each contraction of ν_L and ν_R^T by ε/Q

where v is the electroweak scale, and Q is the momentum of intermediate particles, which is typically ~ 100 MeV.

Since the various operators can arise from new physics at different scales we will distinguish between the corresponding Λ's (new physics scales). Then the amplitude estimates are as follows:

diagrams	dim.	operators	amplitudes
D_ν	5	$\mathcal{O}_\nu$	$1/Q^2v^2\Lambda_\nu$
D_4	7	$\mathcal{O}^{\mathrm{d7}}_{\mathrm{D}_4}$	$1/Qv\Lambda^3_\nu$
	7	$\mathcal{O}^{\mathrm{d7}}_{\mathrm{D}_4}$	$1/Qv\Lambda^3_4$
D'_4	6	$\mathcal{O}_{Ne\phi}$	$1/Qv\Lambda'^2_4\Lambda_\nu$
D_5	7	$\mathcal{O}^{\mathrm{d7}}_{\mathrm{D}_5}$	$1/v^2\Lambda^3_\nu$
	9	$\mathcal{O}^{d9}_{\mathrm{D}_5}$	$1/\Lambda^5_5$
D_6	7	$\mathcal{O}^{\mathrm{d7}}_{\mathrm{D}_6}$	$1/Qv\Lambda^3_{6a}$
	9	$\mathcal{O}^{\mathrm{d9}}_{\mathrm{D}_6}$	$v/Q\Lambda^5_{6b}$
D_7	7	$\mathcal{O}^{\mathrm{d7}}_{\mathrm{D}_7}$	$1/16\pi^2v^2\Lambda^3_{7a}$
	9	$\mathcal{O}^{\mathrm{d9}}_{\mathrm{D}_7}$	$1/\Lambda^5_{7b}$
D_9	9	$\mathcal{O}^{\mathrm{d9}}_{\mathrm{D}_9}$	$1/\Lambda^5_{9a}$
	11	$\mathcal{O}^{\mathrm{d11}}_{\mathrm{D}_9}$	v^2/Λ^7_{9b}

(8.1)

In the above chart we used

$$m_\nu = \frac{v^2}{\Lambda_\nu}, \tag{8.2}$$

and the following definitions

Λ = The new physics scale of each operator,

$$\mathcal{O}^{\mathrm{d7}}_{\mathrm{D}_4} \equiv \{\mathcal{O}_{g4a,b,c}\},$$

$$\mathcal{O}^{\mathrm{d7}}_{\mathrm{D}_6} \equiv \{\mathcal{O}_{3b}, \mathcal{O}_{4a}, \mathcal{O}_{4a}, \mathcal{O}_8\},\ \mathcal{O}^{\mathrm{d9}}_{\mathrm{D}_6} \equiv \{\mathcal{O}_5, \mathcal{O}_6, \mathcal{O}_7\},$$

$$\mathcal{O}^{\mathrm{d7}}_{\mathrm{D}_7} \equiv \mathcal{O}_{g7a},\ \mathcal{O}^{\mathrm{d9}}_{\mathrm{D}_7} \equiv \{\mathcal{O}_{g7b,c,d,e,f,g,h,i,j}\},$$

$$\mathcal{O}^{\mathrm{d9}}_{\mathrm{D}_9} \equiv \{\mathcal{O}_{11b}, \mathcal{O}_{12a}, \mathcal{O}_{14b}, \mathcal{O}_{19}, \mathcal{O}_{20}\}$$

$$\mathcal{O}^{\mathrm{d11}}_{\mathrm{D}_9} \equiv \{\mathcal{O}_{24a}, \mathcal{O}_{28a,c}, \mathcal{O}_{32a}, \mathcal{O}_{36}, \mathcal{O}_{37}, \mathcal{O}_{38}, \mathcal{O}_{47a,d}, \mathcal{O}_{53}, \mathcal{O}_{54a,d}, \mathcal{O}_{55a}, \mathcal{O}_{59}, \mathcal{O}_{60}\}, \tag{8.3}$$

where the superscript dn of $\mathcal{O}^{\mathrm{d}n}_{\mathrm{D}_m}$ indicates the dimension of the operator and the subscript D_m indicates the type of the corresponding Feynman diagram. Notice that, as it was mentioned in Section 7.3, the same Λ_ν for $\mathcal{O}_\nu$ also has been used for $\mathcal{O}^{\mathrm{d7}}_{\mathrm{D}_4}$ and $\mathcal{O}^{\mathrm{d7}}_{\mathrm{D}_5}$ because the heavy physics models inducing these operators also induce $\mathcal{O}_\nu$. Therefore, the limits on Λ_ν can be obtained from more than one diagrams, but the contributions of the heavy physics to $0\nu\beta\beta$ through D_5 and D_7 are negligible compared to the contributions through D_ν.

8.2 Ranges of dominance for each type of graph

Table 8.1 shows the condition that each operator has dominant contribution to the $0\nu\beta\beta$ decay over other operators' contributions. In the table, we have assumed $Q = 100$ MeV and $v = 246$ MeV.

8.3 Limits on the new physics scales from $0\nu\beta\beta$ decay

Using the limit on the effective Majorana-neutrino mass from currently the most sensitive experiment, the limit on the amplitude of $0\nu\beta\beta$ decay can be estimated as

$$\mathcal{A} < 8 \times 10^{-3}\ \mathrm{TeV}^{-5}. \tag{8.4}$$

From this we can obtain the limit on the new physics scale assuming that each new physics is the only contribution to the $0\nu\beta\beta$ decay. We also assume that there is no accidental suppression by the presence of small couplings.

The lower limits on the heavy physics scales are listed in the following chart

diagrams	new physics scales	lower limits in TeV
D_ν	Λ_ν	2×10^{11}
D_4	Λ_4	170
D_5	Λ_5	2.6
D_6	Λ_{6a}	170
	Λ_{6b}	12.5
D_7	Λ_{7a}	2.3
	Λ_{7b}	2.6
D_9	Λ_{9a}	2.6
	Λ_{9b}	2.3

(8.5)

where we have assumed $Q = 100$ MeV and $v = 246$ MeV.

The lower limits on Λ_ν, Λ_{6a}, and Λ_{6b} are so large that the corresponding heavy particles cannot be produced at any collider in the present and near future. All other physics scales are several TeVs and the corresponding heavy particles can be produced at the LHC. The limits on the heavy physics scales generating D_9 were first mentioned in [87]. The observation of $0\nu\beta\beta$ decay will open up the possibility that there are some types of heavy particles that contribute to the $0\nu\beta\beta$ decay and also can be produced at the LHC.

8.4 Discovery limits on new physics scales at the LHC

The effective operators $\mathcal{O}^{\rm d7}_{\rm D_5}$ and $\mathcal{O}^{\rm d9}_{\rm D_5}$ contributing to D_5 can contribute to the same-sign dilepton production in proton-proton collisions

$$p + p \to \ell^+ + \ell^+ + X. \tag{8.6}$$

Reference [91] provides the discovery limits when the processes (8.6) are generated by right-handed neutrino interactions at the LHC. These results can be easily translated into limits on the new physics scale Λ_ν for $\mathcal{O}^{\rm d7}_{\rm D_5}$, and Λ_5 for $\mathcal{O}^{\rm d9}_{\rm D_5}$ for 1, 3 and 10 events.

Then, the upper limits on the new physics scales for the discovery of the same-sign dilepton production by $\mathcal{O}^{\rm d7}_{\rm D_5}$ and $\mathcal{O}^{\rm d9}_{\rm D_5}$ at the LHC are as follows

n	Λ_ν(TeV)	Λ_5(TeV)
10	2.7	1.0
3	3.2	1.2
1	3.9	1.3

(8.7)

Here n is the number of events, and it is assumed that the luminosity of the beam at the LHC is 100 fb^{-1} and $\sqrt{s} = 14$ TeV. As we can see from the chart, the discovery limits of the new physics scales are below the lower bounds on the scales from the $0\nu\beta\beta$ decay.

8.5 Explicit evaluation of the decay rate for $\mathcal{O}_{g5}$

In this section we are going to evaluate the decay rate of $0\nu\beta\beta$ induced by $\mathcal{L}_{g5}$. We are going to follow the calculation in [71].

After ϕ aquires a VEV, eq.(7.17) can be rewritten in the basis of electric-charge eigenfields as follows

$$\begin{aligned}\mathcal{L}_{g5} = &\frac{g}{\sqrt{2}} W^-_\mu (\bar{\Psi}_- \gamma^\mu \Psi_0 - \bar{\Psi}_0 \gamma^\mu \Psi_+) + Y v \bar{e}_L \Psi_- + Y' v \bar{\Psi}_+ e^c_L + \text{H.c.} \\ &- \frac{M_\Psi}{2} \bar{\Psi}_+ \Psi_+ - \frac{M_\Psi}{2} \bar{\Psi}_- \Psi_- - M_\Psi \bar{\Psi}_0 \Psi_0,\end{aligned} \tag{8.8}$$

where $\Psi_- \equiv \Psi_1 + i\Psi_2$, $\Psi_+ \equiv \Psi_1 - i\Psi_2$ and $\Psi_0 \equiv \Psi_3$, which have electric charges -1, -2

and 0 respectively. We integrate out only Ψ_- and Ψ_+ to have the following expression

$$\mathcal{L}_{g5} \sim Yv\frac{g}{\sqrt{2}}(\frac{-i}{M_\Psi})\bar{e}_L W_\mu^- \gamma^\mu \Psi_0 - Y'v\frac{g}{\sqrt{2}}(\frac{-i}{M_\Psi})\bar{\Psi}_0 W_\mu^- \gamma^\mu e_L^c + \text{H.c.}. \tag{8.9}$$

From the above Lagrangian, with the W-hadron current in the Standard Model, we can obtain an effective Lagrangian for $0\nu\beta\beta$ decay as in figure 8.1, which is in the same form as the effective Lagrangian for the standard mechanism

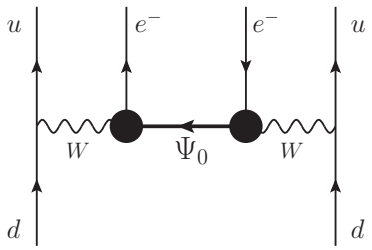

Figure 8.1: $0\nu\beta\beta$ by $\mathcal{O}_{g5}$

$$\mathcal{L}_W^\beta = -i\frac{Yv}{M_\Psi}\frac{G_F}{\sqrt{2}}2(\bar{e}_L\gamma^\mu\Psi_0)j_\mu + i\frac{Y'v}{M_\Psi}\frac{G_F}{\sqrt{2}}2(\bar{\Psi}_0\gamma^\mu e_L^c)j_\mu, \tag{8.10}$$

$$j_\mu \equiv 2\cos\theta_c \bar{u}_L\gamma_\mu d_L, \tag{8.11}$$

where θ_c is the CKM mixing angle.

Following the calculations in [71] we obtain the amplitude for the $0\nu\beta\beta$ decay

$$\begin{aligned}\mathcal{A}_{g5} = iYY'\left(\frac{v}{M_\Psi}\right)^2\left(\frac{G_F}{\sqrt{2}}\right)^2\frac{M_\Psi}{R}\bar{u}(p_1)(1+\gamma^5)C\bar{u}^T(p_2) \\ \times (M_F - g_A^2 M_{\text{GT}})\delta(p_{10}+p_{20}+M'-M),\end{aligned} \tag{8.12}$$

where M and M' are the masses of the initial and final nuclei respectively. Here we neglected the momentum of the final nucleus. Then the above amplitude gives the same decay rate as the standard mechanism with G_F^2 is replaced by $G_F'^2 \equiv YY'(v'/M_\Psi)^2 G_F^2$ and the effective neutrino mass $|\langle m\rangle|$ is replaced by M_Ψ. Here, notice that this does

not imply that the decay rate diverges as $M_\Psi \to \infty$, because M_Ψ is included in other factors too.

The decay rate will then be

$$\Gamma_{0\nu\beta\beta} = \frac{{G'_F}^4 m_e^5}{2(2\pi)^5} M_\Psi^2 \frac{1}{R^2} \left| M_F - g_A^2 M_{GT} \right|^2 F^2(Z) \times \frac{1}{15}(\varepsilon_0^5 + 10\varepsilon_0^4 + 40\varepsilon_0^3 + 60\varepsilon_0^2 + 30\varepsilon_0), \tag{8.13}$$

where the constants and the functions are defined as follows [71]

$$\begin{aligned} m_e &\equiv \text{Electron mass}, \\ R &\equiv \text{The radius of the initial nucleus}, \\ g_A &\equiv 1.25, \text{Axial constant}, \\ F(Z) &\equiv \frac{2\pi\alpha(Z+2)}{1-\exp[-2\pi\alpha(Z+2)]} \\ &= \text{Fermi factor of the coulomb corrections}, \\ \varepsilon_0 &\equiv \frac{1}{m_e}(M_{\text{initial nucleus}} - M_{\text{final nucleus}} - 2m_e) \\ &= \text{Kinetic energy of the final electrons}, \end{aligned} \tag{8.14}$$

M_F and M_{GT} are the nuclear matrix elements. M_F is negligible compared to M_{GT} [73]. In the reference [73], M_{GT} is calculated for the cases in which the mass of the mediating particle is light or heavy. When the standard mechanism is mediated by a heavy particle of mass M_Ψ, the nuclear matrix element is proportional to $1/M_\Psi^2$

$$M_{GT} \sim \frac{R}{48r}\left(\frac{M_A}{M_\Psi}\right)^2 e^{-M_A r\{(M_A r)^3 + 3(M_A r)^2 + 3(M_A r)\}}, \tag{8.15}$$

where r is the distance between the neutrons, and the dipole form factor mass of the nucleon $M_A \sim 0.9$ GeV.

Table 8.1: The condition of the dominance of the amplitude by each operator over another operator. All scales are in TeV units. If the condition in the cell which is n-th from the left of the table and m-th from the top (n,m) is given, the amplitude in the cell (n,1) is larger than the amplitudes in the cell (1,m).

S\L	$\mathcal{A}^{\rm d7}_{\rm D_4}$	$\mathcal{A}^{\rm d9}_{\rm D_5}$	$\mathcal{A}^{\rm d7}_{\rm D_6}$	$\mathcal{A}^{\rm d9}_{\rm D_6}$	$\mathcal{A}^{\rm d7}_{\rm D_7}$	$\mathcal{A}^{\rm d9}_{\rm D_7}$	$\mathcal{A}^{\rm d9}_{\rm D_9}$	$\mathcal{A}^{\rm d11}_{\rm D_9}$
$\mathcal{A}_\nu$	$\Lambda_4 < .029\Lambda_\nu^{\frac{1}{3}}$	$\Lambda_5 < .14\Lambda_\nu^{\frac{1}{5}}$	$\Lambda_{6a} < .029\Lambda_\nu^{\frac{1}{3}}$	$\Lambda_{6b} < .068\Lambda_\nu^{\frac{1}{5}}$	$\Lambda_{7a} < .0004\Lambda_\nu^{\frac{1}{3}}$	$\Lambda_{7b} < .014\Lambda_\nu^{\frac{1}{7}}$	$\Lambda_{9a} < .014\Lambda_\nu^{\frac{1}{5}}$	$\Lambda_{9b} < .032\Lambda_\nu^{\frac{1}{7}}$
$\mathcal{A}^{\rm d7}_{\rm D_4}$		$\Lambda_5 < .12\Lambda_4^{\frac{3}{5}}$	$\Lambda_{6a} < \Lambda_4$	$\Lambda_{6b} < .57\Lambda_4^{\frac{3}{5}}$	$\Lambda_{7a} < .014\Lambda_4$	$\Lambda_{7b} < .12\Lambda_4^{\frac{3}{5}}$	$\Lambda_{9a} < .12\Lambda_4^{\frac{3}{5}}$	$\Lambda_{9b} < .15\Lambda_4^{\frac{3}{7}}$
$\mathcal{A}^{\rm d9}_{\rm D_5}$	$\Lambda_4 < 34\Lambda_{5b}^{\frac{5}{3}}$		$\Lambda_{6a} < 34\Lambda_{5b}^{\frac{5}{3}}$	$\Lambda_{6b} < 4.8\Lambda_{5b}$	$\Lambda_{7a} < .47\Lambda_{5b}^{\frac{5}{3}}$	$\Lambda_{7b} < \Lambda_{5b}$	$\Lambda_{9a} < \Lambda_{5b}$	$\Lambda_{9b} < .67\Lambda_{5b}^{\frac{5}{7}}$
$\mathcal{A}^{\rm d7}_{\rm D_6}$	$\Lambda_4 < \Lambda_{6a}$	$\Lambda_5 < .12\Lambda_{6a}^{\frac{3}{5}}$		$\Lambda_{6b} < .57\Lambda_{6a}^{\frac{3}{5}}$	$\Lambda_{7a} < .014\Lambda_{6a}$	$\Lambda_{7b} < .12\Lambda_{6a}^{\frac{3}{5}}$	$\Lambda_{9a} < .12\Lambda_{6a}^{\frac{3}{5}}$	$\Lambda_{9b} < .15\Lambda_{6a}^{\frac{3}{7}}$
$\mathcal{A}^{\rm d9}_{\rm D_6}$	$\Lambda_4 < 2.5\Lambda_{6b}^{\frac{5}{3}}$	$\Lambda_5 < .21\Lambda_{6b}$	$\Lambda_{6a} < 2.5\Lambda_{6b}^{\frac{5}{3}}$		$\Lambda_{7a} < .035\Lambda_{6b}^{\frac{5}{3}}$	$\Lambda_{7b} < .21\Lambda_{6b}$	$\Lambda_{9a} < .21\Lambda_{6b}$	$\Lambda_{9b} < .22\Lambda_{6b}^{\frac{5}{7}}$
$\mathcal{A}^{\rm d7}_{\rm D_7}$	$\Lambda_4 < 73\Lambda_{7a}$	$\Lambda_5 < 1.6\Lambda_{7a}^{\frac{3}{5}}$	$\Lambda_{6a} < 73\Lambda_{7a}$	$\Lambda_{6b} < 7.5\Lambda_{7a}^{\frac{3}{5}}$		$\Lambda_{7b} < 1.6\Lambda_{7a}^{\frac{3}{5}}$	$\Lambda_{9a} < 1.6\Lambda_{7a}^{\frac{3}{5}}$	$\Lambda_{9b} < .92\Lambda_{7a}^{\frac{3}{7}}$
$\mathcal{A}^{\rm d9}_{\rm D_7}$	$\Lambda_4 < 34\Lambda_{7b}^{\frac{5}{3}}$	$\Lambda_5 < \Lambda_{7b}$	$\Lambda_{6a} < 34\Lambda_{7b}^{\frac{5}{3}}$	$\Lambda_{6b} < 4.8\Lambda_{7b}$	$\Lambda_{7a} < .47\Lambda_{7b}^{\frac{5}{3}}$		$\Lambda_{9a} < \Lambda_{7b}$	$\Lambda_{9b} < .67\Lambda^{\frac{5}{7}}$
$\mathcal{A}^{\rm d9}_{\rm D_9}$	$\Lambda_4 < 34\Lambda_{9a}^{\frac{5}{3}}$	$\Lambda_5 < \Lambda_{9a}$	$\Lambda_{6a} < 34\Lambda_{9a}^{\frac{5}{3}}$	$\Lambda_{6b} < 4.8\Lambda_{9a}$	$\Lambda_{7a} < .47\Lambda_{9a}^{\frac{5}{3}}$	$\Lambda_{7b} < \Lambda_{9a}$		$\Lambda_{9b} < .67\Lambda_{9a}^{\frac{5}{7}}$
$\mathcal{A}^{\rm d11}_{\rm D_9}$	$\Lambda_4 < 88\Lambda_{9b}^{\frac{7}{3}}$	$\Lambda_5 < 1.8\Lambda_{9b}^{\frac{7}{5}}$	$\Lambda_{6a} < 88\Lambda_{9b}^{\frac{7}{3}}$	$\Lambda_{6b} < 8.4\Lambda_{9b}^{\frac{7}{5}}$	$\Lambda_{7a} < 1.2\Lambda_{9b}^{\frac{7}{3}}$	$\Lambda_{7b} < 1.8\Lambda_{9b}^{\frac{7}{5}}$	$\Lambda_{9a} < 1.8\Lambda_{9b}^{\frac{7}{5}}$	

Chapter 9

Conclusions of Part II

The observation of $0\nu\beta\beta$ decay will tell us if neutrinos are Majorana particles and it also opens up the possibility of new physics and provide the constraints on the new physics scales. If the $0\nu\beta\beta$ decay is generated by only the standard mechanism, the amplitude of the decay is proportional to the effective Majorana-neutrino mass which depends on the Majorana-mass eigenvalues of light neutrinos, the CP-phases and Majorana phases of the lepton mixing matrix. However, it is possible that the $0\nu\beta\beta$ decay can also be generated by various effective vertices induced from new physics models.

In Part 2, we discussed mechanisms for the $0\nu\beta\beta$ decay, effective operators and possible new physics models for the new mechanisms as follows:

(i) We listed all possible tree-level Feynman diagrams with effective vertices contributing to $0\nu\beta\beta$ decay. These diagrams include Standard Model vertices and a lepton number violating vertex. We also considered diagrams containing the standard Majorana mass insertion and a lepton-number-conserving effective vertex. But the contributions of the lepton-number-conserving effective vertices were

negligible compared to the lepton-number-violating vertices.

(ii) We listed the effective operators generating the effective vertices contributing to the $0\nu\beta\beta$ decay.

(iii) We found possible types of new physics with heavy particles generating the effective operators at tree level. In this work, we especially considered the heavy physics generating the effective vertices involving W bosons. Among the effective operators contributing to the diagram D_7, dim-7 operator is not generated at tree level but the dim-9 operator can be generated at tree level. The heavy physics models inducing D_9 were considered in the reference [87].

(iv) We estimated the amplitude of the $0\nu\beta\beta$ decay for each effective operator. For a dim-7 operator contributing to D_5 diagram, we calculated the amplitude of the $0\nu\beta\beta$ explicitly. Based on the amplitude estimates, we presented a table in which we provided the condition for the dominance of each operator's contribution to the $0\nu\beta\beta$ decay over other operators' contributions.

(v) By using the most strict experimental limit on the amplitude of the $0\nu\beta\beta$ decay, We estimated the lower limit of each new physics scale. We found that there are heavy particles whose energy scale limits are within several TeVs, which means that some of these heavy particles can generate the $0\nu\beta\beta$ decay and also can be produced at the LHC. The heavy particles that contribute to D_5 but not to D_ν at tree level were

$$\Phi_{02},\ \Phi_{\frac{1}{2}\frac{3}{2}},\ \Psi_{\frac{1}{2}\frac{1}{2}},\ X_{01},\ X_{11},\ X_{\frac{1}{2}\frac{3}{2}}, \tag{9.1}$$

where Φ_{IY}, Ψ_{IY}, and X_{IY} indicate a heavy scalar, a heavy fermion, and a heavy vector with isospin I and hypercharge Y respectively. All these heavy particles

may be produced at the LHC but a definite statement in this respect requires a complete model. The above set of heavy particles includes doubly charged scalar and vector particles.

(vi) We also obtained the discovery limits on the new physics scales for same-sigh dilepton production at the LHC.

Bibliography

[1] Alberto Aparici, Kyungwook Kim, Arcadi Santamaria, and Jose Wudka. Right-handed neutrino magnetic moments. *Phys. Rev. D*, 80(1):013010, Jul 2009.

[2] Jose Wudka. Electroweak effective lagrangians. *Int. J. Mod. Phys.*, 9A:2301–2362, Feb. 1994.

[3] Howard Georgi. On-shell effective field theory. *Nucl. Phys. B*, 361(2):339–350, September 1991.

[4] Aneesh Manohar and Howard Georgi. Chiral quarks and the non-relativistic quark model. *Nuclear Physics B*, 234(1):189 – 212, 1984.

[5] D. P. Roy. Eighty years of neutrino physics. *Physics News*, 39(3):51, 2009.

[6] M.C. Gonzalez-Garcia and Michele Maltoni. Phenomenology with massive neutrinos. *Phys. Rep.*, 460(1-3):1–129, April 2008.

[7] Y. Fukuda et al. (SK Collaboration). Evidence for oscillation of atmospheric neutrinos. *Phys. Rev. Lett.*, 81(8):1562–1567, Aug 1998.

[8] M. H. Ahn et al. (K2K Collaboration). Measurement of neutrino oscillation by the K2K experiment. *Phys. Rev. D*, 74(7):072003, Oct 2006.

[9] D. G. Michael et al. (MINOS Collaboration). Observation of muon neutrino disappearance with the MINOS detectors in the NuMI neutrino beam. *Phys. Rev. Lett.*, 97(19):191801, Nov 2006.

[10] L. Wolfenstein. Neutrino oscillations in matter. *Phys. Rev. D*, 17(9):2369–2374, May 1978.

[11] S. Mikheyev and A. Y. Smirnov. *Yad. Fiz.*, 42:1441, 1985.

[12] Q. R. Ahmad et al. (SNO Collaboration). Direct evidence for neutrino flavor transformation from neutral-current interactions in the Sudbury Neutrino Observatory. *Phys. Rev. Lett.*, 89(1):011301, Jun 2002.

[13] S. N. Ahmed et al. (SNO Collaboration). Measurement of the total active ^{8}B solar neutrino flux at the Sudbury Neutrino Observatory with enhanced neutral current sensitivity. *Phys. Rev. Lett.*, 92(18):181301, May 2004.

[14] K. Eguchi et al. (KL Collaboration). First results from KamLAND: Evidence for reactor antineutrino disappearance. *Phys. Rev. Lett.*, 90(2):021802, Jan 2003.

[15] T. Araki et al. (KL Collaboration). Measurement of neutrino oscillation with KamLAND: Evidence of spectral distortion. *Phys. Rev. Lett.*, 94(8):081801, Mar 2005.

[16] S. Abe et al. (KL Collaboration). Precision measurement of neutrino oscillation parameters with KamLAND. *Phys. Rev. Lett.*, 100(22):221803, Jun 2008.

[17] M. Apollonio et al. (CHOOZ Collaboration). Search for neutrino oscillations on a long base-line at the CHOOZ nuclear power station. *The European Physical Journal C - Particles and Fields*, 27:331–374, 2003. 10.1140/epjc/s2002-01127-9.

[18] M. C. Gonzalez-Garcia and Carlos Pena-Garay. Three-neutrino mixing after the first results from K2K and KamLAND. *Phys. Rev. D*, 68(9):093003, Nov 2003.

[19] Steven Weinberg. Baryon- and lepton-nonconserving processes. *Phys. Rev. Lett.*, 43(21):1566–1570, Nov 1979.

[20] Peter Minkowski. $\mu \to e\gamma$ at a rate of one out of 10^9 muon decays? *Physics Letters B*, 67(4):421 – 428, 1977.

[21] P. Ramond. The familiy group in grand unified theories. *arXiv:hep-ph/9809459*, 1998.

[22] M. Gell-Mann, P. Ramond, and R. Slansky. Supergravity. in Proceedings of the Supergravity Workshop at Stony Brook, edited by P. Van Nieuwenhuizen and D. Z. Freedman (North-Holland, Amsterdam, 1979).

[23] T. Yanagida. in Proceedings of the Workshop on the Baryon Number of the Universe and Unified Theories, edited by Osamu Sawada and Akio Sugamoto (National Lab for High Energy Physics, Tsukuba, Japan, 1979).

[24] R. N. Mohapatra and G. Senjanovic. Neutrino mass and spontaneous parity nonconservation. *Phys. Rev. Lett.*, 44(14):912–915, Apr 1980.

[25] Ernest Ma. Pathways to naturally small neutrino masses. *Phys. Rev. Lett.*, 81(6):1171–1174, Aug 1998.

[26] I. Yu. Kobzarev, B. V. Martemyanov, L. B. Okun, and M. G. Shchepkin. The phenomenology of neutrino oscillations. *Sov. J. Nucl. Phys.*, 32:823, 1980.

[27] S. M. Bilenky, J. Hosek, and S. T. Petcov. On the oscillations of neutrinos with Dirac and Majorana masses. *Physics Letters B*, 94(4):495 – 498, 1980.

[28] T. P. Cheng and Ling-Fong Li. Neutrino masses, mixings, and oscillations in $SU(2) \times U(1)$ models of electroweak interactions. *Phys. Rev. D*, 22(11):2860–2868, Dec 1980.

[29] J. Schechter and J. W. F. Valle. Neutrino masses in $SU(2) \times U(1)$ theories. *Phys. Rev. D*, 22(9):2227–2235, Nov 1980.

[30] R. N. Mohapatra and P. B. Pal. Massive neutrinos in physics and astrophysics. *World Sci. Lect. Notes Phys.*, 41, 1991.

[31] R. N. Mohapatra and G. Senjanovic. Neutrino masses and mixings in gauge models with spontaneous parity violation. *Phys. Rev. D*, 23(1):165–180, Jan 1981.

[32] G. Lazarides, Q. Shafi, and C. Wetterich. Proton lifetime and fermion masses in an $SO(10)$ model. *Nuclear Physics B*, 181(2):287 – 300, 1981.

[33] M. Magg and Ch. Wetterich. Neutrino mass problem and gauge hierarchy. *Physics Letters B*, 94(1):61 – 64, 1980.

[34] M. Fukugita and T. Yanagida. Barygenesis without grand unification. *Physics Letters B*, 174(1):45 – 47, 1986.

[35] Alberto Aparici, Arcadi Santamaria, and Jose Wudka. A model for right-handed neutrino magnetic moments. *arXiv:0911.4103v1 [hep-ph]*, November 2009.

[36] Howard Georgi. Generalized dimensional analysis. *Physics Letters B*, 298(1-2):187 – 189, 1993.

[37] Mark Terwort. Searchs for GMSB at the LHC. *arXiv:0805.2524v2*, 2008.

[38] Piotr Zalewski. Search for GMSB NLSPs at LHC. *arXiv:0710.2647v1*, 2007.

[39] Damien Prieur. GMSB SUSY models with non pointing photons signatures in ATLAS at the LHC. *arXiv:hep-ph/0507083v1*, 2005.

[40] K. Nakamura et al. (Particle Data Group). Review of particle physics. *J. Phys. G*, 37(075021), 2010.

[41] Gary J. Feldman and Robert D. Cousins. Unified approach to the classical statistical analysis of small signals. *Phys. Rev. D*, 57(7):3873–3889, Apr 1998.

[42] P. Abreu et al. (DELPHI Collaboration). Search for new phenomena using single photon events at LEP1. *Z. Phys. C*, 74:577–586, 1997. 10.1007/s002880050421.

[43] P. Abreu et al. (DELPHI Collaboration). Search for neutral heavy leptons produced in Z decays. *Z. Phys. C*, 74:57–71, 1997. 10.1007/s002880050370.

[44] O. Adriani et al. (L3 Collaboration). Search for isosinglet neutral heavy leptons in Z^0 decays. *Phys. Lett. B*, 295(3-4):371 – 382, 1992.

[45] M. Z. Akrawy et al. (OPAL COllaboration). Limits on neutral heavy lepton production from Z^0 decay. *Physics Letters B*, 247(2-3):448 – 457, 1990.

[46] J. Abdallah et al. (DELPHI Collaboration). Photon events with missing energy in e^+e^- collisions at $\sqrt{s}$ = 130 to 209 GeV. *Eur. Phys. J. C*, 38:395–411, 2005. 10.1140/epjc/s2004-02051-8.

[47] P. Achard et al. (L3 Collaborations). Single- and multi-photon events with missing energy in e^+e^- collisions at LEP. *Phys. Lett. B*, 587(1-2):16 – 32, 2004.

[48] G. Abbiendi et al. (OPAL Collaboration). Search for anomalous photonic events with missing energy in e^+e^- collisions at $\sqrt{s}$ = 130, 136 and 183 GeV. *Eur. Phys. J. C*, 8:23–40, 1999. 10.1007/s100529901083.

[49] G. Abbiendi et al. (OPAL Collaboration). Search for unstable heavy and excited leptons at LEP2. *Eur. Phys. J. C*, 14:73–84, 2000. 10.1007/s100520000345.

[50] V. Castellani and S. degl'Innocenti. Stellar evolution as a probe of neutrino properties. *Astrophys. J.*, 402:574–578, January 1993.

[51] M. Catelan, J. A. de Freitas Pacheco, and J. E. Horvath. The helium-core mass at the helium flash in low-mass red giant stars: Observations and theory. *Astrophys. J.*, 461:231, April 1996.

[52] M. Haft, G. Raffelt, and A. Weiss. Standard and nonstandard plasma neutrino emission revisited. *Astrophys. J.*, 425:222–230, April 1994.

[53] G. G. Raffelt. Core mass at the helium flash from observations and a new bound on neutrino electromagnetic properties. *Astrophys. J.*, 365:559–568, December 1990.

[54] G. G. Raffelt. New bound on neutrino dipole moments from globular-cluster stars. *Phys. Rev. Lett.*, 64(24):2856–2858, Jun 1990.

[55] G. Raffelt and A. Weiss. Nonstandard neutrino interactions and the evolution of red giants. *Astron. Astrophys.*, 264:536–546, 1992.

[56] A. Heger, A. Friedland, M. Giannotti, and V. Cirigliano. The impact of neutrino magnetic moments on the evolution of massive stars. *Astrophys. J.*, 696:608–619, 2009.

[57] G. G. Raffelt. *Stars as Laboratories for Fundamental Physics: The Astrophysics of Neutrinos, Axions, and Other Weakly Interacting Particles*. University Of Chicago Press, Chicago, IL, 1996.

[58] Naoki Iwamoto, Letao Qin, Masataka Fukugita, and Sachiko Tsuruta. Neutrino magnetic moment and neutron star cooling. *Phys. Rev. D*, 51(2):348–352, Jan 1995.

[59] Scott Dodelson and Lawrence M. Widrow. Sterile neutrinos as dark matter. *Phys. Rev. Lett.*, 72(1):17–20, Jan 1994.

[60] Xiangdong Shi and George M. Fuller. New dark matter candidate: Nonthermal sterile neutrinos. *Phys. Rev. Lett.*, 82(14):2832–2835, Apr 1999.

[61] U. Seljak, A. Makarov, P. McDonald, and H. Trac. Can sterile neutrinos be the dark matter? *Phys. Rev. Lett.*, 97(19):191303, Nov 2006.

[62] Matteo Viel, Julien Lesgourgues, Martin G. Haehnelt, Sabino Matarrese, and Antonio Riotto. Can sterile neutrinos be ruled out as warm dark matter candidates? *Phys. Rev. Lett.*, 97(7):071301, Aug 2006.

[63] Julien Lesgourgues and Sergio Pastor. Massive neutrinos and cosmology. *Phys. Rpt.*, 429(6):307 – 379, 2006.

[64] A. Melchiorri, O. Mena, S. Palomasres-Ruiz, S. Pascoli, A. Slosar, and M. Sorel. Sterile neutrinos in light of recent cosmological and oscillation data: a multi-flavor scheme approach. *J. Cosmol. Astropart. Phys.*, 01(036), 2009.

[65] A. D. Sakharov. Violation of CP invariance, C asymmetry, and baryon asymmetry of the universe. *JETP Lett.*, 5:24, 1967.

[66] A. Pilaftsis. The little review on leptogenesis. *J. Phys. Conf. Ser.*, 171(1), 2009.

[67] Laura Covi, Esteban Roulet, and Francesco Vissani. CP violating decays in leptogenesis scenarios. *Physics Letters B*, 384(1-4):169 – 174, 1996.

[68] Marion Flanz, Emmanuel A. Paschos, Utpal Sarkar, and Jan Weiss. Baryogenesis through mixing of heavy Majorana neutrinos. *Phys. Lett. B*, 389:693–699, 1996.

[69] Apostolos Pilaftsis. CP violation and baryogenesis due to heavy Majorana neutrinos. *Phys. Rev. D*, 56(9):5431–5451, Nov 1997.

[70] Apostolos Pilaftsis and Thomas E. J. Underwood. Resonant leptogenesis. *Nuclear Physics B*, 692(3):303 – 345, 2004.

[71] S. M. Bilenky and S. T. Petcov. Massive neutrinos and neutrino oscillations. *Rev. Mod. Phys.*, 59(3):671–754, Jul 1987.

[72] Masaru Doi, Tsuneyuki Kotani, and Eiichi Takasugi. Double beta decay and Majorana neutrino. *Prog. Theor. Phys. Suppl.*, 83, 1985.

[73] W. C. Haxton and G. J. Stephenson. Double beta decay. *Prog. Part. Nucl. Phys.*, 12:409 – 479, 1984.

[74] J. Schechter and J. W. F. Valle. Neutrinoless double-β decay in $SU(2) \times U(1)$ theories. *Phys. Rev. D*, 25(11):2951–2954, Jun 1982.

[75] Eiichi Takasugi. Can the neutrinoless double beta decay take place in the case of Dirac neutrinos? *Phys. Lett. B*, 149(4-5):372 – 376, 1984.

[76] Jose F. Nieves. Dirac and pseudo-Dirac neutrinos and neutrinoless double beta decay. *Physics Letters B*, 147:375 – 379, 1984.

[77] H. Primakoff and S. P. Rosen. Double beta decay. *Pep. Prog. Phys.*, 22:121, 1959.

[78] H.V. Klapdor-Kleingrothaus, A. Dietz, L. Baudis, G. Heusser, I.V. Krivosheina, B. Majorovits, H. Paes, H. Strecker, V. Alexeev, A. Balysh, A. Bakalyarov, S.T. Belyaev, V.I. Lebedev, and S. Zhukov. Latest results from the heidelberg-moscow double beta decay experiment. *The European Physical Journal A - Hadrons and Nuclei*, 12:147–154, 2001. 10.1007/s100500170022.

[79] S. M. Bilenky, C. Giunti, J. A. Grifols, and E. Masso. Absolute values of neutrino masses: status and prospects. *Phys. Rpt.*, 379(2):69 – 148, 2003.

[80] Dusan Budjas, Marik Barnabe Heider, Oleg Chkvorets, Nikita Khanbekov, and Stefan Schonert. Pulse shape discrimination studies with a broad-energy germanium detector for signal identification and background suppression in the GERDA double beta decay experiment. *JINST*, 4:P10007, 2009.

[81] H. V. Klapdor-Kleingrothaus, A. Dietz, H. L. Harney, and I. V. Krivosheina. Evidence for neutrinoless double beta decay. *Mod. Phys. Lett. A*, 16(37):2409, 2001.

[82] H. V. Klapdor-Kleingrothaus, A. Dietz, I. V. Krivosheina, and O. Chkvorets. Data acquisition and analysis of the ^{76}Ge double beta experiment in Gran Sasso 1990-2003. *Nucl. Instrum. Methods A*, 522(3):371 – 406, 2004.

[83] H.V Klapdor-Kleingrothaus, I.V Krivosheina, A Dietz, and O Chkvorets. Search for neutrinoless double beta decay with enriched ^{76}Ge in Gran Sasso 1990-2003. *Physics Letters B*, 586(3-4):198 – 212, 2004.

[84] H. V. Klapdor-Kleingrothaus and I. V. Krivosheina. The evidence for the observation of $0\nu\beta\beta$ decay: The identification of $0\nu\beta\beta$ events from the full spectra. *Mod. Phys. Lett. A*, 21:1547–1566, 2006.

[85] S. M. Bilenky. Neutrinoless double beta-decay. *Phys. Part. Nucl.*, 41:690–715, 2010.

[86] Andre de Gouvea and James Jenkins. Survey of lepton number violation via effective operators. *Phys. Rev. D*, 77(1):013008, Jan 2008.

[87] K. S. Babu and C. N. Leung. Classification of effective neutrino mass operators. *Nucl. Phys. B*, 619(1-3):667–689, 2001.

[88] Francisco del Aguila, Shaouly Bar-Shalom, Amarjit Soni, and Jose Wudka. Heavy Majorana neutrinos in the effective Lagrangian description: Application to hadron colliders. *Phys. Lett. B*, 670(4-5):399 – 402, 2009.

[89] W. Buchmuller and D. Wyler. Effective lagrangian analysis of new interactions and flavour conservation. *Nucl. Phys. B*, 268(3-4):621 – 653, 1986.

[90] S. Bar-Shalom, F. del Aguila, Kyungwook Kim, A. Santamaria, and J. Wudka. Heavy physics effects on neutrinoless double-beta decay. In preparation.

[91] A. Ali, A.V. Borisov, and N.B. Zamorin. Same-sign dilepton production via heavy Majorana neutrinos in proton-proton collisions, arXiv:hep-ph/0112043v2. 2001.

[92] A. Abulencia et al. (CDF Collaboration). Inclusive search for new physics with like-sign dilepton events in $p\bar{p}$ collisions at $\sqrt{s} = 1.96$ TeV. *Phys. Rev. Lett.*, 98(22):221803, Jun 2007.

[93] John M. Cornwall, David N. Levin, and George Tiktopoulos. Derivation of gauge invariance from high-energy unitarity bounds on the S matrix. *Phys. Rev. D*, 10(4):1145–1167, Aug 1974.

[94] Benjamin W. Lee, C. Quigg, and H. B. Thacker. Weak interactions at very high energies: The role of the higgs-boson mass. *Phys. Rev. D*, 16(5):1519–1531, Sep 1977.

[95] Ernest Ma and Utpal Sarkar. Neutrino masses and leptogenesis with heavy higgs triplets. *Phys. Rev. Lett.*, 80(26):5716–5719, Jun 1998.

[96] Georg G. Raffelt. Limits on neutrino electromagnetic properties – an update. *Phys. Rpt.*, 320(1-6):319 – 327, 1999.

Appendix A

Decay rates and cross sections

We present the relevant formulas for decay rates and cross sections used in Part 1.

A.1 Notations and definitions

We have used the following notations and definitions:

$$c_W \equiv \cos\theta_W,\ s_W \equiv \sin\theta_W,\ \alpha \equiv \frac{e^2}{4\pi}, \tag{A.1a}$$

$$\zeta_{ij} = |\zeta_{ij}|e^{i\delta_{ij}}, \tag{A.1b}$$

$$q_f \equiv \text{charge of fermion } f, \tag{A.1c}$$

$$a_f \equiv t_3(f) = \text{eigenvalue of } t_3 \text{ of } f,\ t_3 = \frac{1}{2}\sigma^3, \tag{A.1d}$$

$$v_f \equiv t_3(f)(1 - 4|q_f|s_W^2), \tag{A.1e}$$

$$\lambda(a,b,c) \equiv a^2 + b^2 + c^2 - 2ab - 2ac - 2bc, \tag{A.1f}$$

$$\begin{aligned} f_Z(m_Z, m_i, m_j) \equiv & \frac{\sqrt{\lambda(m_Z^2, m_i^2, m_j^2)}}{m_Z^6} \\ & \times [m_Z^2(m_Z^2 + m_i^2 + m_j^2 - 6m_i m_j \cos 2\delta_{ij}) - 2(m_i^2 - m_j^2)^2], \end{aligned} \tag{A.1g}$$

$$\chi(s) \equiv \frac{s}{s - m_Z^2 + im_Z\Gamma(Z \to N_1 N_2)}, \tag{A.1h}$$

$$\eta_f(s) \equiv 4q_f^2 c_W^2 - 4q_f v_f \mathrm{Re}\{\chi(s)\} + \frac{v_f^2 + a_f^2}{c_W^2}|\chi(s)|^2. \tag{A.1i}$$

A.2 Decay rates for $Z^0 \to N_i N_j$

The decay rate of the Z^0 boson into heavy Majorana neutrinos is

$$\Gamma(Z^0 \to N_i + N_j) = \frac{2|\zeta_{ij}|^2}{3\pi} s_W^2 m_Z^3 f_Z(m_Z, m_i, m_j), \tag{A.2}$$

where f_Z is defined in (A.1g) and $f_Z(m_Z, 0, 0) = 1$.

A.3 N_2 decay rates

The decay rates of the heaviest neutrino into a neutral boson and a lighter heavy neutrino are

$$\Gamma(N_2 \to N_1 + \gamma) = \frac{2}{\pi} c_W^2 |\zeta_{12}|^2 m_2^3 \left(1 - \frac{m_1^2}{m_2^2}\right)^3, \tag{A.3}$$

$$\Gamma(N_2 \to N_1 + Z^0) = \frac{2}{\pi} s_W^2 |\zeta_{12}|^2 m_2^3 f_2(m_Z, m_1, m_2), \tag{A.4}$$

with

$$f_2(m_Z, m_1, m_2) = -\frac{m_Z^6}{2m_2^6} f_Z(m_Z, m_1, m_2),$$

$$f_2(0, 0, m_2) = 1. \tag{A.5}$$

A.4 N_1 decay rates

The lightest heavy neutrinos N_1 can only decay into the SM particles. If $m_1 > m_Z$ the dominant decays proceed through the SM interactions induced by the mixing of heavy-light neutrinos:

$$\Gamma(N_1 \to \ell_\beta^- + W^+) = \frac{1}{16} |\varepsilon_W^\beta|^2 \frac{\alpha m_1^3}{s_W^2 m_W^2} \left(1 - \frac{m_W^2}{m_1^2}\right)^2 \left(1 + 2\frac{m_W^2}{m_1^2}\right), \tag{A.6}$$

where β is a flavor index and ε_W characterizes the mixing of heavy-light neutrinos in W boson couplings, which is of the order of $\sqrt{m_\nu/m_N}$.

For $N_1 \to \nu_\beta + Z^0$ decays we obtain

$$\Gamma(N_1 \to \nu_\beta + Z^0) = \frac{1}{16} |\varepsilon_Z^{\beta 1}|^2 \frac{\alpha m_1^3}{s_W^2 c_W^2 m_Z^2} \left(1 - \frac{m_Z^2}{m_1^2}\right)^2 \left(1 + 2\frac{m_Z^2}{m_1^2}\right), \tag{A.7}$$

where ε_Z is defined as ε_W but for Z^0 boson couplings. Notice that since $m_W = c_W m_Z$ the two decay widths are equal up to phase space factors and differences in the mixing factors ε_Z and ε_W. However, we have two decay channels into W's, $N_1 \to e^- + W^+$ and

$N_1 \to e^+ + W^-$, and only one into Z's (we already took into account that the ν_β are Majorana particles; should we treat them as Weyl particles, we have two decay channels and the sum over them gives the same result).

If $m_1 > m_H$ the N_1 can also decay into Higgs bosons. The decay rate of $N_1 \to \nu + H$ is

$$\Gamma(N_1 \to \nu_\beta + H) = \frac{|Y_\nu^{\beta 1}|^2 m_1}{32\pi}\left(1 - \frac{m_H^2}{m_1^2}\right)^2. \tag{A.8}$$

If we use $\varepsilon \simeq M_D M_N^{-1}$, $M_D = Y_\nu v/\sqrt{2}$ and $\alpha/(s_W^2 m_W^2) = 1/(\pi v^2)$ to rewrite

$$\frac{|\varepsilon|^2 \alpha m_1^3}{s_W^2 m_W^2} \sim |Y_\nu|^2 \frac{m_1}{2\pi v^2}, \tag{A.9}$$

then in the limit $m_1 \gg m_H, m_W, m_Z$, the above three decay rates are identical, i.e., $\Gamma(N_1 \to \ell_\beta^- + W^+) = \Gamma(N_1 \to \nu_\beta + Z^0) = \Gamma(N_1 \to \nu_\beta + H)$. This is required by the equivalence theorem [93, 94] which states that, in this limit, the calculation could have been performed in the theory before spontaneous symmetry breaking; in that theory, all the fields except the N are massless, there is no heavy-light mixing and the N's decay into the doublet of leptons and the Higgs scalar doublet through the standard model Yukawa couplings. However for moderate m_1, the phase space factors are important, in particular, $\Gamma(N_1 \to \nu_\beta + H)$ decreases rapidly as m_1 approaches m_H.

If $m_1 < m_W$, N_1 dominantly decays into a light neutrino and a photon by the magnetic moment coupling, which is suppressed by the heavy-light mixing. The decay rate is

$$\Gamma(N_1 \to \nu_\beta + \gamma) = \frac{2}{\pi}|\varepsilon_\gamma^{\beta 1}|^2 c_W^2 m_1^3, \tag{A.10}$$

where ε_γ is a parameter that characterizes the strength of the $N_1 - \nu_\beta - \gamma$ interaction and it is of the order of $(1/\Lambda_{\rm NP})\sqrt{m_\nu/m_N}$.

A.5 Cross section for $e^+e^- \to N_1 + N_2 + X$

If we neglect the interactions involving light neutrinos, the cross sections at the LEP and ILC are

$$\sigma(e^+ + e^- \to N_1 + N_2) = \frac{2\alpha}{3}|\zeta_{12}|^2 f_Z(\sqrt{2}, m_1, m_2)\eta_f(s), \tag{A.11}$$

where η_f is defined in (A.1i) and $f = e$.

A.6 Partonic cross section for $p + p \to N_1 + N_2 + X$

To calculate $\sigma(p + p \to N_1 + N_2 + X)$, We need to calculate the differential cross sections for $q + \bar{q} \to N - 1 + N_2$, which proceed through the electroweak-moment interaction and are dominated by γ and Z^0 exchange:

$$\begin{aligned}
&\frac{d\hat{\sigma}}{d\Omega}(q + \bar{q} \to N_1 + N_2) \\
&= \frac{\alpha}{6\pi}|\zeta_{12}|^2 \eta_q(\hat{s}) \frac{\sqrt{\lambda(\hat{s}, m_1^2, m_2^2)}}{\hat{s}^3} \\
&\quad \times [(m_1^2 + m_2^2)(\hat{s} + 2\hat{t}) - 2\hat{t}(\hat{s} + \hat{t}) - (m_1^4 + m_2^4) - 2\hat{s}m_1 m_2 \cos 2\delta_{12}],
\end{aligned} \tag{A.12}$$

where $\hat{s}$ and $\hat{t}$ are the Mandelstam variables for the partonic collision in the center of mass frame of the quarks, and $\eta_q(\hat{s})$ is defined in (A.1i) with $f = q$. Then the total partonic cross section is obtained by integration of the angular variables and the result is the same as (A.11) with an additional factor 1/3 due to color and with q_f, a_f, v_f appropriate for $f = u, d$.

A.7 Decay rates for $H \to N_1 + N_2$

The operator $(\phi^\dagger\phi)\overline{\nu_R^c}\xi\nu_R$ can induce new decay modes for the Higgs boson. We found

$$\begin{aligned}\Gamma(H \to N_1 + N_2) =& \frac{v^2}{2\pi m_H^3}|\xi_{12}|^2\sqrt{\lambda(m_H^2, m_1^2, m_2^2)} \\ & \times [(m_H^2 - m_1^2 - m_2^2) - 2m_1 m_2 \cos 2\delta'_{12}],\end{aligned} \tag{A.13}$$

where $\xi_{ij} = |\xi_{ij}|e^{i\delta'_{ij}}$ and $\langle\phi^{(0)}\rangle = v/\sqrt{2}$.